

MICHIGAN STATE UNIVERSITY LIBRARIES

3 1293 00550 9785

This is to certify that the

thesis entitled

Digital Simulation of Field Oriented (Vector)

Control of Induction Machine Using PWM

Voltage Source Inverter Without Speed Sensor

presented by

Chungsong Hwang

has been accepted towards fulfillment of the requirements for

M·S degree in <u>Electrical</u> Engineering

Major professor

Date 23 Oct 88

MSU is an Affirmative Action/Equal Opportunity Institution

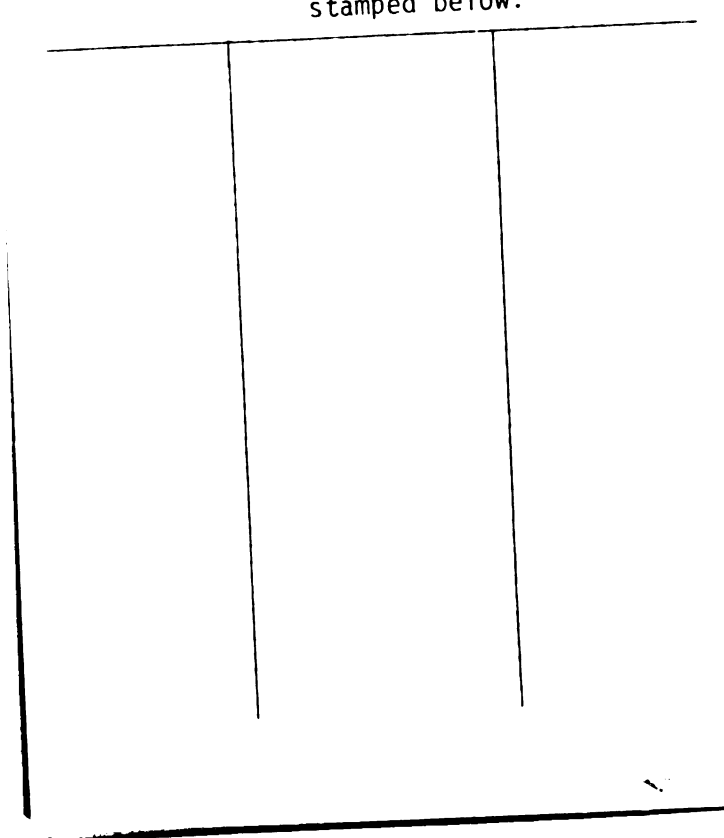
O-7639

LIBRARY Michigan State University



RETURNING MATERIALS:
Place in book drop to remove this checkout from your record. FINES will be charged if book is returned after the date

stamped below.



Digital Simulation of Field Oriented (Vector) Control of Induction Machine Using PWM Voltage Source Inverter Without Speed Sensor

Ву

Chungsang Hwang

A THESIS

Submitted to
Michigan State University
in partial fulfillment of the requirements
for the degree of

MASTER OF SCIENCE

Department of Electrical Engineering

1988

ABSTRACT

Digital Simulation of Field Oriented (Vector) Control of Induction Machine Using PWM Voltage Source Inverter Without Speed Sensor

By

Chungsang Hwang

This thesis describes the simulation of a control scheme using the principle of the field orientation for the control of a voltage source inverter-fed induction motor. The control principle is explained, followed by an algorithm to simulate components of the system. The scheme uses only current sensors without speed sensor and allows high performanace speed and torque control. Compensation for flux deviation is proposed, which is necessary for system stability and control accuracy. The results of simulation show that the speed and torque control accuracy is good in terms of dynamic and steady state. Also, a microprocessor-based PWM method is described, which is based on treating the inverter as a logic system in real time.

To my mother

ACKNOWLEDGEMENT

I wish to express my sincere appreciation to my major advisor, Dr. Elias G. Strangas, for his guidance and encourgement in the course of this research.

Also, I would like to thank to my committee member, Dr. Robert A. Schlueter and Dr. Michael Shanblatt, for their suggestions.

Finally, I owe a special thanks to my mother for her encourgement and support.

TABLE OF CONTENTS

CHAPTER		PAGE
I.	INTRODUCTION	. 1
II.	PRINCIPLE OF FIELD-ORIENTED CONTROL	. 2
	2.1 Mathematical Model of the Symmetrical Induction Motor	. 2
	2.2 Field-Oriented Coordinate Transformation	. 4
	2.3 Dynamic Characteristics	. 6
III.	CONTROL SCHEME	. 8
IV.	INDIRECT ROTOR EMF AND SLIP CALCULATION FOR SPEED SENSORLESS SYSTEM	. 11
	4.1 Differential Equations in Stationary Reference Frame	. 11
	4.2 Slip Calculation from Flux	. 13
	4.3 Rotor EMF Method to Calculate Slip Using Stator Components	. 14
	4.4 Analysis of Transient Rotor Flux Calculation	. 18
v.	COMPENSATION OF FLUX DEVIATION	. 20
	5.1 Voltage Control Method	. 20
	5.2 Φ _{rq} Zero Control	. 23
VI.	FLUX POSITION CONTROLLER AND COORDINATE TRANSFORMATION	. 25
	6.1 Flux Position Controller	. 25
	6.2 Coordinate Transformation	. 26
VII	DI CONTROLLED	20

VIII.	GATE	PULSE GENERATION	30
	8.1	Pulse Width Modulation for 3-Phase Inverter	30
	8.2	Generation of Pulses from Frequency, Magnitude and Phase Angle	31
	8.3	Harmonics due to PWM	33
	8.4	Hardware Implementation	39
viiii.	RESUI	LTS AND CONCLUSIONS	42
	9.1	Simulation Results	42
		9.1.1 Acceleration without Load	45
		9.1.2 Step Load after Transient	50
		9.1.3 Reference Speed Reversal without Load	55
	9.2	Conclusions	60
	T.TST	OF REFERENCES	61

LIST OF FIGURES

FIGURE		PAGE
1	Equivalent circuit of an induction motor	. 2
2	Angular relationship of current and flux linkage vectors	. 5
3	Induction machine model in rotating frame of reference	. 6
4	Control scheme diagram	. 10
5	Induction motor equivalent circuit in the rotor flux fixed frame	. 12
6	Computation of slip frequency	. 17
7	A diagram for the estimation of the rotor flux and slip frequency	. 19
8	Compensation for flux deviation	. 24
9	A diagram of flux position controller	. 26
10	The principle of PWM signal generation	. 30
11	Three phase bridge inverter	. 33
12	Switching function of a PWM inverter	. 34
13	PWM generation	. 35
14	Hardware configuration of PWM generation	. 39
15	Flow chart of the main program	. 43
16	Flow chart of the controller	. 44
17	The d-axis stator current from standstill to 377 rad/sec	. 46
18	The q-axis stator current from standstill to 377 rad/sec	46

19	Rotor flux current from standstill	
	to 377 rad/sec	47
20	Speed from standstill to 377 rad/sec	47
21	Torque from standstill to 377 rad/sec	48
22	The d-axis rotor flux from standstill to 377 rad/sec	. 48
23	The q-axis rotor flux from standstill to 377 rad/sec	. 49
24	Flux compensation from standstill to 377 rad/sec	49
25	Step response of d-axis current. startup to 377 rad/sec	51
26	Step response of q-axis current. startup to 377 rad/sec	51
27	Step response of rotor flux current. startup to 377 rad/sec	52
28	Step response of speed. startup to 377 rad/sec	52
29	Step response of torque. startup to 377 rad/sec	53
30	Step response of d-axis rotor flux. startup to 377 rad/sec	53
31	Step response of q-axis rotor flux. startup to 377 rad/sec	54
32	Step response of flux compensation. startup to 377 rad/sec	54
33	Speed reversal of d-axis current from 377 to -377 rad/sec	56
34	Speed reversal of q-axis current from 377 to -377 rad/sec	56
35	Speed reversal of rotor flux current	57

36	Speed reversal of speed from 377 to -377 rad/sec	57
37	Speed reversal of torque from 377 to -377 rad/sec	58
38	Speed reversal of d-axis rotor flux from 377 to -377 rad/sec	58
39	Speed reversal of q-axis rotor flux from 377 to -377 rad/sec	59
40	Speed reversal of flux compensation from 377 to -377 rad/sec	59

LIST OF TABLES

TABLE		PAG	ΞE
1	Motor parameters	42	2

CHAPTER I

INTRODUCTION

The dynamic properties of an induction motor as a control plant can be described by a set of nonlinear differential equations. These equations relate the electrical quantities, currents and voltages of the motor, with the mechanical quantities of torque and speed. The control of such a plant becomes complicated because of the intricate coupling between all the control inputs.

This problem can be overcome by the control of field-oriented quantities which reduce the control of an AC induction motor to that of a separately excited DC motor.

Various control schemes have been proposed for the voltage source inverterfed drive system [1,2] in recent years.

However, in field-oriented drives actual speed and rotor position must be known to the controllers. This requires a speed sensor mounted on the rotor shaft and signal wiring from the speed sensor to the inverter cubicle. They increase the cost of the drive system in addition to reducing the overall reliability of the system.

In order to overcome these problems, several control schemes without speed sensor have been presented [2-4].

In the scheme proposed here, two compensations for the simulation, one for flux deviation to make flux ϕ_{rq} zero and the other for decoupling voltage and current components, are considered. Also a flux position controller has been incorporated which, determines the desired position of the flux to establish the required field components.

CHAPTER II

PRINCIPLE OF FIELD-ORIENTED CONTROL

The field-oriented control for induction motor is based on establishing two orthogonal components of the stator current, i_{sd} on the axis of the rotor magnetic field and i_{sq} orthogonal to it. i_{sd} excites the magnetic field and i_{sq} produces torque. This control scheme treats the induction motor as like it were a DC motor, and equally controllable. Unlike a DC motor, the two components of the stator current are not stationary. Instead they rotate at synchronous speed and their frame of reference is tied to the rotor magnetizing current.

2.1 Mathematical Model of the Symmetrical Induction Motor

Figure 1 shows the equivalent induction motor circuit.

Let us define a space vector of the current as

$$\underline{i}_{s}(t) = i_{s1}(t) + i_{s2}(t)e^{j\frac{2}{3}\pi} + i_{s3}(t)e^{j\frac{4}{3}\pi}.$$
 (1)

The stator terminal voltage is defined accordingly as

$$\underline{u_s}(t) = u_{s1}(t) + u_{s2}(t)e^{j\frac{2}{3}\pi} + u_{s3}(t)e^{j\frac{4}{3}\pi}.$$
 (2)

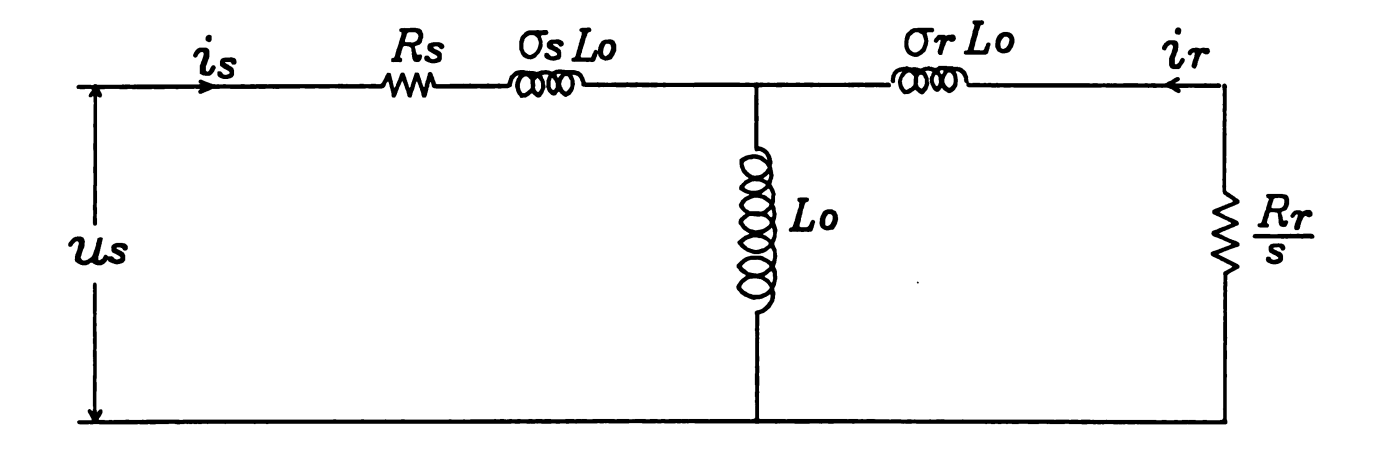


Figure 1. Equivalent circuit of an induction motor.

The equations of the symmetrical induction motor with a short-circuited rotor circuit, in a stator reference frame, are defined as follows:

$$R_{s}\underline{i}_{s}(t) + L_{s}\frac{d}{dt}(\underline{i}_{s}(t)) + L_{o}\frac{d}{dt}(\underline{i}_{r}(t)e^{j\,\epsilon}) = \underline{u}_{s}(t), \qquad (3)$$

$$R_r \underline{i}_r(t) + L_r \frac{d}{dt}(\underline{i}_r(t)) + L_o \frac{d}{dt}(\underline{i}_s(t)e^{-j\varepsilon}) = 0, \qquad (4)$$

$$J\frac{d\omega_{r}}{dt} = T_{d} - T_{l} = \frac{2}{3}L_{o} \operatorname{Im} \left\{ i_{s}(t)(i_{r}(t)e^{j\epsilon})^{*} \right\} - T_{l} , \qquad (5)$$

$$\frac{d\varepsilon}{dt} = \omega_r . ag{6}$$

Where

$$L_s = (1 + \sigma_s) L_o ,$$

$$L_r = (1 + \sigma_r) L_o ,$$

$$\sigma = 1 - \frac{1}{(1 + \sigma_s)(1 + \sigma_r)} ,$$

and

ω, is the rotor angular frequency,

o, is the stator leakage factor,

 σ_s is the rotor leakage factor,

σ is the total leakage factor,

ε is the angle of rotation,

 L_o is the coefficient of mutual inductivity,

 T_d is the driving torque,

 T_l is the load torque.

2.2 Field-Oriented Coordinate Transformation

This model can be transformed into the rotating reference frame at synchronous speed to obtain the relation between field-oriented quantities.

Since the rotor currents can not be measured in cage rotor motors, it is appropriate to replace $i_r(t)$ by an equivalent quantity that could be measured with stator based sensing equipment.

For this purpose, a magnetizing current vector, $i_{mr}(t)$, representing the rotor flux reference can be defined as follows:

$$\underline{i}_{mr}(t) = \underline{i}_{s}(t) + (1 + \sigma_{r})\underline{i}_{r}(t)e^{j\varepsilon} = i_{mr}(t)e^{j\rho(t)}$$
(7)

and

$$\frac{d\rho}{dt} = \omega \tag{8}$$

where

ω is stator angular frequency.

In the frame of reference defined by $\underline{i}_{mr}(t)$, the component i_{sd} of $\underline{i}_{s}(t)$ parallel to the rotor flux and the component i_{sq} , perpendicular to it, are related to $\underline{i}_{s}(t)$ as (see Figure 2)

$$\underline{i}_{s}(t) e^{-j\rho} = i_{sd} + ji_{sq} . \tag{9}$$

The voltage vector $\underline{u}_{r}(t)$ is related to its components as

$$\underline{u}_{s}(t) = (u_{sd} + ju_{sq}) e^{j\phi}. \tag{10}$$

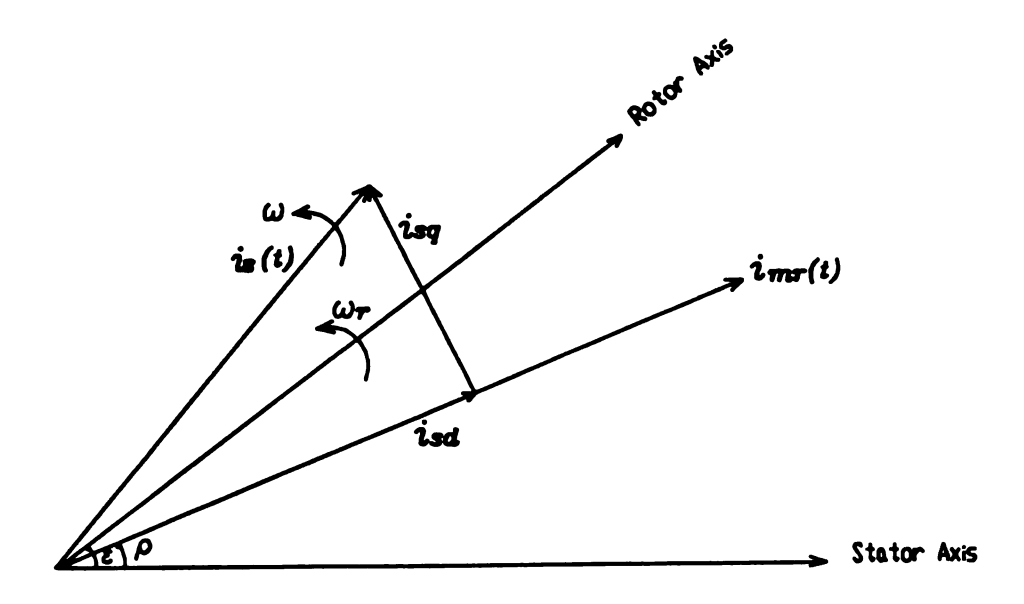


Figure 2. Angular relationship of current and flux linkage vectors.

By transforming the machine model expressed in the stator frame with definitions in (7)-(10), yields

$$\sigma T_s \frac{di_{sd}}{dt} + i_{sd} = \frac{u_{sd}}{R_s} - (1 - \sigma)T_s \frac{i_{mr}}{dt} + \sigma T_s \omega i_{sq} , \qquad (11)$$

$$\sigma T_s \frac{di_{sq}}{dt} + i_{sq} = \frac{u_{sq}}{R_s} - (1 - \sigma)T_s \omega i_{mr} - \sigma T_s \omega i_{sd} , \qquad (12)$$

$$T_r \frac{di_{mr}}{dt} + i_{mr} = i_{sd} , \qquad (13)$$

$$\frac{d\rho}{dt} = \omega = \omega_r + \frac{i_{sq}}{T_r i_{mr}}, \qquad (14)$$

and

$$J\frac{d\omega_{r}}{dt} = T_{d} - T_{l} = \frac{2}{3} \frac{L_{o}}{(1+\sigma_{r})} i_{mr} i_{sq} - T_{l} . \tag{15}$$

Where

$$T_s = \frac{L_s}{R_s} ,$$

$$T_r = \frac{L_r}{R_r} ,$$

and

J is the inertia of the machine.

2.3 Dynamic Characteristics

The machine model in the rotating reference frame was essentially reduced to two flow paths, one for the flux governed by expression (13) with i_{sd} as the control input and the other for the torque governed by expression (15) with control input i_{sq} together with ϕ_{mr} , the rotor flux (see Figure 3).

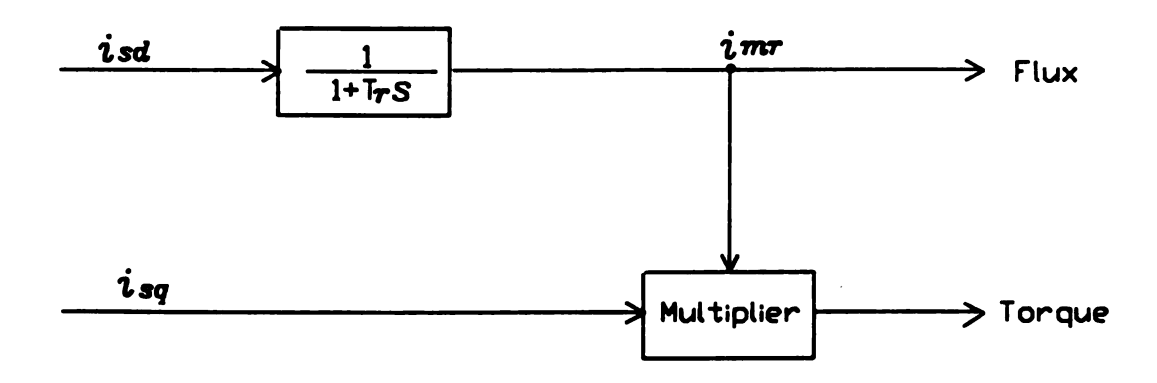


Figure 3. Induction machine model in rotating frame of reference.

The flux path in this model is similar to the field circuit and the torque path is similar to the armature circuit of a separately excited DC motor.

As it is normally done in a DC motor, the flux level in the machine should be maintained at a maximum level depending on the AC voltage available and the operating flux density of the motor. It should be maximum up to the base speed, above which it may be weakened.

The speed control can be imposed on i_{sq} and the flux control on i_{sd} . When reference values for i_{sd} and i_{sq} are calculated, reference for the field oriented quantities u_{sd} and u_{sq} are established.

CHAPTER III

CONTROL SCHEME

The control scheme consists of speed, torque and flux controllers. The flux controller, which operates on the difference between the rotor flux reference and the actual rotor flux, sets the reference for i_{sd} which is denoted by i_{sd}^* . Similarly, the speed error $(\omega_r^* - \omega_r)$ serves as the input to the speed controller, which sets the reference for the torque. This reference value when divided by the magnitude of the actual flux vector gives i_{sd}^* .

To achieve a fast response drive system, the corresponding voltage has to be impressed on the motor. The reference voltage, u_{sd}^{*} and u_{sq}^{*} , can be obtained from (11) and (13), which define the relation between the stator current and the terminal voltage in the field coordinates.

Since these equations include motor-parameters, they will produce errors because of the variation of the motor-parameters due to the temperature and the accuracy with which they are measured. Hence, a closed-loop control system is required for i_{sd} and i_{sq} , which is achieved by the flux controller and torque controller as shown in Figure 4.

Once the manipulated values u_{sd}^* and u_{sq}^* are determined, they are to be properly positioned in the stationary reference frame.

Equation (14) defines the desired slip. Actual slip is calculated with the indirect rotor EMF method discussed in the next section.

The output of the flux controller gives the incremental value $\Delta \rho$ of ρ , which, when added to the actual flux position ρ , gives the desired position, $\rho_o = \rho + \Delta \rho$, of the flux vector.

Knowing the desired position of the flux vector, the terminal voltage of the stationary reference can be calculated. This is then converted to the three phase quantities serving as the reference voltage for the inverter (see Chapter VI).

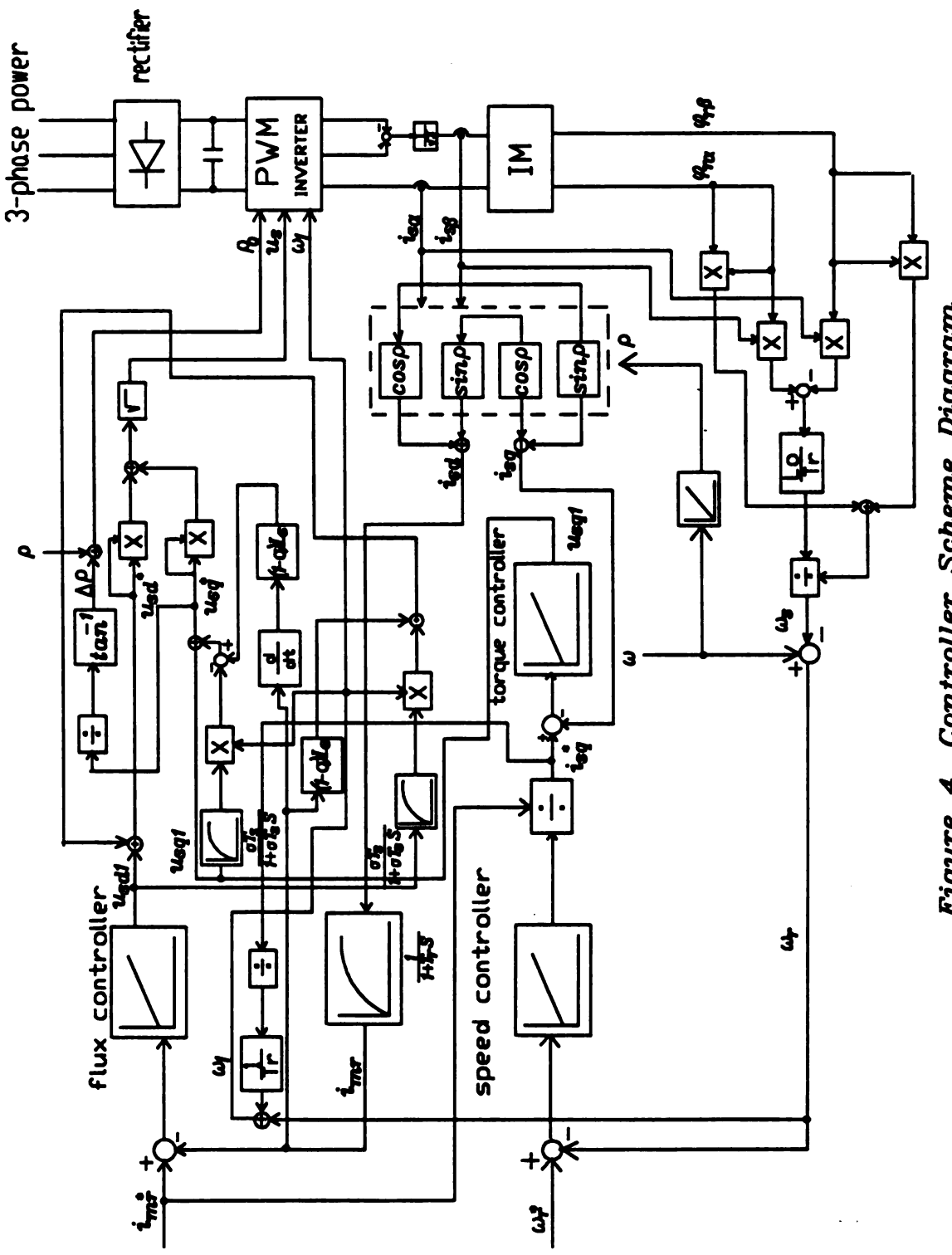


Figure 4. Controller Scheme Diagram

CHAPTER IV

INDIRECT ROTOR EMF AND SLIP CALCULATION FOR SPEED SENSORLESS SYSTEM

4.1 Differential Equations in Stationary Reference Frame

An improved method of computing the actual slip was developed [2], based on the differential equations describing the machine behavior in the stationary reference frame.

As state variables are used the flux components in the stator fixed rectangular coordinates (α, β) , while the currents in these coordinates are auxiliary variables. Based on the corresponding circuits (Figure.5), the state equations are:

$$\frac{d}{dt}\phi_{s\alpha} = u_{s\alpha} - R_s i_{s\alpha} , \qquad (16)$$

$$\frac{d}{dt}\phi_{r\alpha} = -R_r i_{r\alpha} - \omega_r \phi_{r\beta} , \qquad (17)$$

$$\frac{d}{dt}\phi_{r\beta} = -R_r i_{r\beta} + \omega_r \phi_{r\alpha} , \qquad (18)$$

$$\frac{d}{dt}\phi_{s\beta} = u_{s\beta} - R_s i_{s\beta} . \tag{19}$$

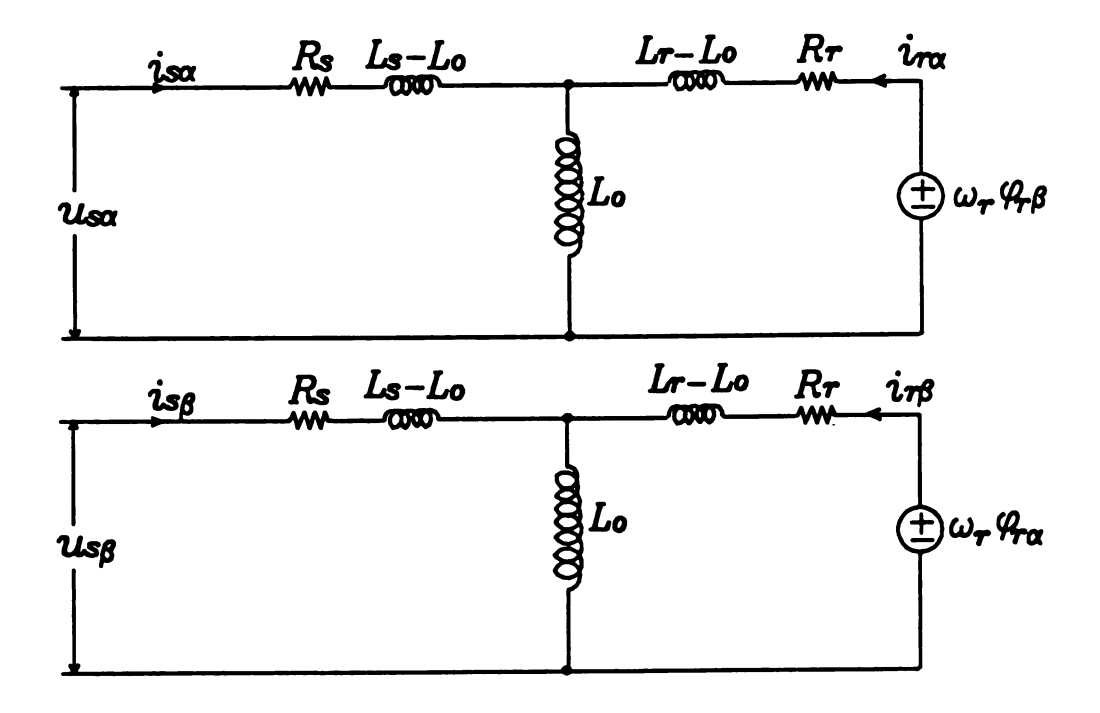


Figure 5. Induction motor equivalent circuit in the rotor flux fixed frame.

In matrix form

$$\mathbf{i} = k \, \mathbf{\phi} = (L)^{-1} \mathbf{\phi} = \frac{1}{L_s L_r + L_o^2} \begin{bmatrix} L_r \, \phi_{s\alpha} - L_o \, \phi_{r\alpha} \\ L_s \, \phi_{r\alpha} - L_o \, \phi_{s\alpha} \\ L_r \, \phi_{s\beta} - L_o \, \phi_{r\beta} \\ L_s \, \phi_{r\beta} - L_o \, \phi_{s\beta} \end{bmatrix}, \tag{20}$$

where

$$\mathbf{i} = (i_{s\alpha}, i_{r\alpha}, i_{s\beta}, i_{r\beta})^{T},$$

$$\mathbf{\phi} = (\phi_{s\alpha}, \phi_{r\alpha}, \phi_{s\beta}, \phi_{r\beta})^{T},$$

Taking derivatives

$$\phi_{r\alpha} \phi_{r\alpha}^{\cdot} + \phi_{r\beta} \phi_{r\beta}^{\cdot} = 0.$$

Then,

$$\dot{\phi_{r\alpha}} = -\frac{\phi_{r\beta}}{\phi_{r\alpha}}\dot{\phi_{r\beta}}, \qquad (28)$$

and

$$\dot{\phi_{r\beta}} = -\frac{\phi_{r\alpha}}{\phi_{r\beta}}\dot{\phi_{r\alpha}}.$$
 (29)

Substituting (29) in (25) gives

$$\omega = \frac{\frac{-\phi_{r\alpha}^{2}}{\phi_{r\beta}}\phi_{r\dot{\alpha}} - \phi_{r\alpha}^{2}\phi_{r\beta}}{\phi_{r\alpha}^{2} + \phi_{r\beta}^{2}}$$

$$=-\frac{\dot{\phi}_{r\alpha}}{\dot{\phi}_{r\beta}}.$$
 (30)

Substituting (28) in (25) gives

$$\omega = \frac{\dot{\phi_{r\beta}} \, \phi_{r\alpha} + \frac{\phi_{r\beta}^2}{\phi_{r\alpha}} \, \dot{\phi_{r\beta}}}{\phi_{r\alpha}^2 + \phi_{r\beta}^2}$$

$$= \frac{\dot{\phi_{r\beta}}}{\phi_{r\alpha}}.$$
(31)

From (30) and (31) and with slowly changing flux

$$\phi_{r\alpha} \approx \frac{1}{\omega} \dot{\phi_{r\beta}} \,, \tag{32}$$

and

$$\phi_{r\beta} \approx \frac{-1}{\omega} \dot{\phi_{r\alpha}} \,. \tag{33}$$

$$L = diag \left\{ \begin{bmatrix} L_s & L_o \\ L_o & L_r \end{bmatrix} \begin{bmatrix} L_s & L_o \\ L_o & L_r \end{bmatrix} \right\},\,$$

and

$$L^{-1} = \frac{1}{(L_s L_r + L_o^2)} \operatorname{diag} \left\{ \begin{bmatrix} L_r & -L_o \\ -L_o & L_s \end{bmatrix} \begin{bmatrix} L_r & -L_o \\ -L_o & L_s \end{bmatrix} \right\}.$$

4.2 Slip Calculation from Flux

The torque expressed in rotor quantities is

$$T_d = n_p \left(i_{r\alpha} \phi_{r\beta} - i_{r\beta} \phi_{r\alpha} \right) \tag{21}$$

where

 n_p is the number of pole pairs

and

$$\omega_r = \omega - \omega_s . \tag{22}$$

Substituting (17), (19), and (22) in (21) gives

$$T_d = \frac{n_p}{R_r} \left[(\omega_s - \omega) (\phi_{r\alpha}^2 + \phi_{r\beta}^2) + (\phi_{r\beta}^2 \phi_{r\alpha} - \phi_{r\alpha}^2 \phi_{r\beta}) \right]$$

and

$$\omega_s - \omega = \frac{R_r T_d}{n_p (\phi_{r\alpha}^2 + \phi_{r\beta}^2)} - \frac{\dot{\phi_r \beta} \phi_{r\alpha} - \dot{\phi_r \alpha} \phi_{r\beta}}{(\phi_{r\alpha}^2 + \phi_{r\beta}^2)}.$$

Calculating ω from Figure 2 gives

$$\rho = \tan^{-1} \frac{\phi_{r\beta}}{\phi_{r\alpha}} ,$$

and

$$\frac{d\rho}{dt} = \omega = \frac{\phi_{r\alpha} \dot{\phi_{r\beta}} - \phi_{r\beta} \dot{\phi_{r\alpha}}}{\phi_{r\alpha}^2 + \phi_{r\beta}^2}.$$

Finally

$$T_d = n_p \, \omega_s \, \left(\frac{1}{R_r}\right) (\phi_r \alpha^2 + \phi_r \beta^2) \,, \tag{23}$$

$$\omega_s = \frac{T_d R_r}{n_p (\phi_{r\alpha}^2 + \phi_{r\beta}^2)}, \qquad (24)$$

$$\omega = \frac{\phi_{r\beta} \phi_{r\alpha} - \phi_{r\alpha} \phi_{r\beta}}{\phi_{r\alpha}^2 + \phi_{r\beta}^2}.$$
 (25)

The torque also can be expressed by stator currents and rotor flux as

$$T_d = n_p \frac{L_o}{L_r} (\phi_{r\alpha} i_{s\beta} - \phi_{r\beta} i_{s\alpha}). \qquad (26)$$

Substituting (26) in (24) yields

$$\omega_s = \frac{L_o}{L_r} R_r \frac{\phi_{r\alpha} i_{s\beta} - \phi_{r\beta} i_{s\alpha}}{(\phi_{r\alpha}^2 + \phi_{r\beta}^2)}. \tag{27}$$

4.3 Rotor EMF Method to Calculate Slip Using Stator Components

Equation (27) is not adequate to calculate slip because it contains rotor components which are not measurable. Instead we derive the slip equation using stator current components which are measurable. A useful expression is obtained if $|\phi_r|^2 = \phi_r \alpha^2 + \phi_r \beta^2$ can be made constant, or, only changing slowly as

$$\phi_{r\alpha}^2 + \phi_{r\beta}^2 = constant$$
.

 $\phi_{r\alpha}$, $\phi_{r\beta}$ can be interpreted as the components of the rotor EMF in the (α, β) frame.

Substituting (32),(33) in (27) yields

$$\omega_{s} = R_{r} \frac{L_{o}}{L_{r}} \frac{\frac{\phi_{r\beta}}{\omega} i_{s\beta} + \frac{\phi_{r\alpha}}{\omega} i_{s\alpha}}{\frac{\phi_{r\alpha}^{2} + \phi_{r\beta}^{2}}{\omega^{2}}}$$

$$= R_{r} \frac{L_{o}}{L_{r}} \frac{\omega (\phi_{r\beta}^{2} i_{s\beta} + \phi_{r\alpha}^{2} i_{s\alpha})}{\phi_{r\alpha}^{2} + \phi_{r\beta}^{2}}.$$

So,

$$\omega_s \approx \omega R_r \frac{L_o}{L_r} \frac{e_{r\beta} i_{s\beta} + e_{r\alpha} i_{s\alpha}}{e_{r\alpha}^2 + e_{r\beta}^2}.$$
 (34)

where

$$\dot{\phi}_{r\alpha} = e_{r\alpha}$$

and

$$\dot{\phi_{r\beta}} = e_{r\beta} .$$

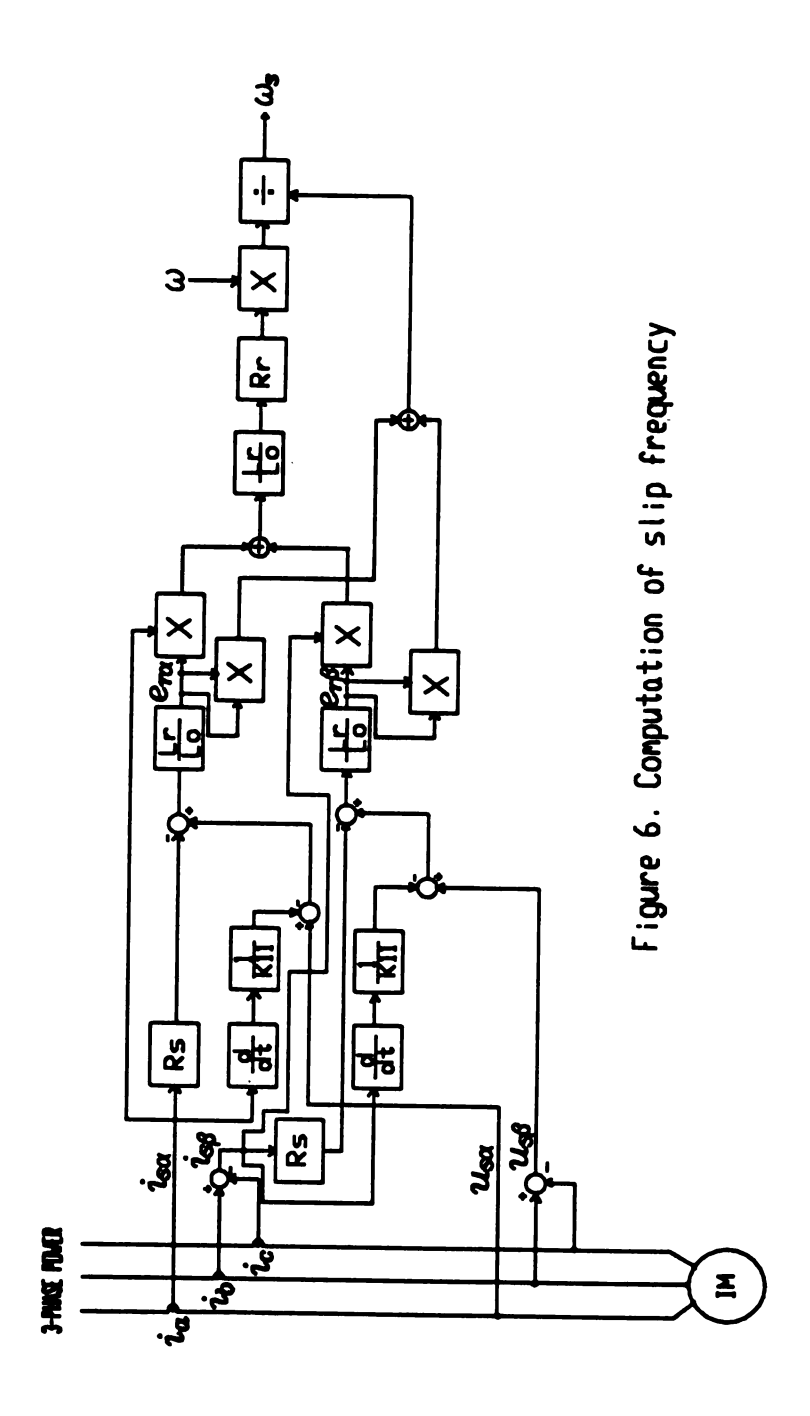
The rotor EMF $e_{r\alpha}$, $e_{r\beta}$ can be obtained from measured stator quantities and Figure 6 shows an implementation of the following equations:

$$e_{r\alpha} = \frac{L_r}{L_o} (u_{s\alpha} - R_s i_{s\alpha} - \frac{1}{k_{11}} \frac{di_{s\alpha}}{dt}), \qquad (35)$$

$$e_{r\beta} = \frac{L_r}{L_o} (u_{s\beta} - R_s i_{s\beta} - \frac{1}{k_{11}} \frac{di_{s\beta}}{dt})$$
 (36)

where

$$k_{11} = \frac{L_r}{L_r - L_0^2} \ .$$



Equations (34), (35) and (36) are the key equations for calculating the actual slip from measured stator quantities instead as the difference between ω and ω .

By introducing the rotor EMF method, it is possible to eliminate the speed sensor which is used to measure the rotor speed ω .

4.4 Analysis of Transient Rotor Flux Calculation

In the previous section, we assumed that $|\phi_r|^2 = \text{constant}$, which is suitable for the steady state. Now let us consider rotor flux in transient state. From (7) we get

$$\underline{i}_{mr}(t) = \underline{i}_{\sigma}(t) + (1 + \sigma_r)\underline{i}_{\sigma}(t)e^{j\varepsilon}$$
(7)

$$= \underline{i}_{\varepsilon}(t) + \frac{L_r}{L_o} \underline{i}_r(t) e^{j\varepsilon}. \tag{37}$$

where

$$(1+\sigma_r)L_o = L_r .$$

We can define

$$\phi_r(t) = L_r \underline{i}_r(t) e^{j \cdot \xi} + L_o \underline{i}_s(t)$$

$$= L_o(\underline{i}_s(t) + \frac{L_r}{L_o} \underline{i}_r(t) e^{j \cdot \xi}) .$$
(38)

Substituting (37) in (38) gives

$$\Phi_r(t) = L_o i_{mr}(t) . \tag{39}$$

and

$$\omega_s = \frac{1}{T_r} \frac{L_o}{\phi_r} i_{sq} . \tag{14}$$

Substituting (39) in (13) and (14) gives

$$T_r \frac{d\phi_r}{dt} + \phi_r = L_o i_{sd} , \qquad (39)$$

and

$$\omega_s = \frac{1}{T_r} \frac{L_o}{\phi_r} i_{sq} . \tag{40}$$

From equations (39) and (40) we can calculate rotor flux ϕ , and slip frequency ω_s during the transient. The estimation flux diagram for the rotor flux and slip frequency is shown in Figure 7.

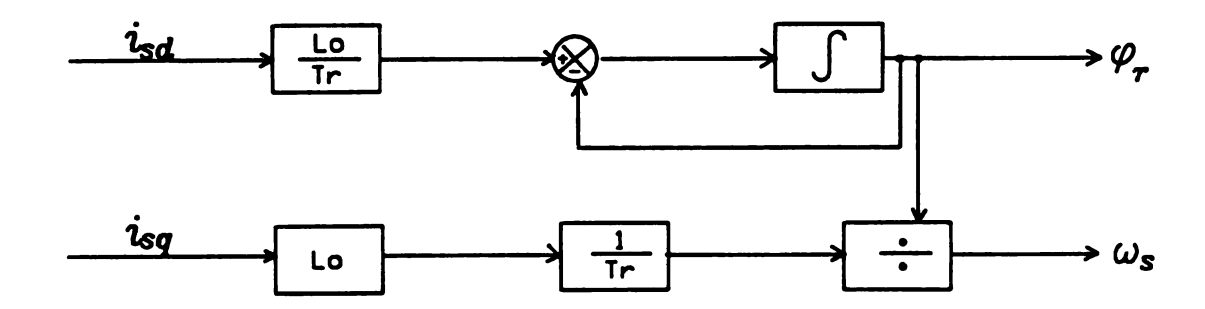


Figure 7. A diagram for the estimation of the rotor flux and slip frequency.

CHAPTER V

COMPENSATION OF FLUX DEVIATION

5.1 Voltage Control Method

If the flux ϕ_{rd} is kept constant and the flux ϕ_{rq} kept zero, the torque is generated without delay in proportion to the current component i_{sd} . However, there will be a flux deviation due to the various disturbances. Therefore, it is important to find a control measure which makes ϕ_{rq} zero. This method is denoted as ϕ_{rq} zero control (see 5.2). The voltage equation of a induction machine [4] is given by the following formula in rectangular d-q coordinates with stator angular frequency ω .

From equation (3) we get

$$u_s e^{j \, \cot} = R_s i_s e^{j \, \cot} + L_s \frac{d}{dt} (i_s e^{j \, \cot}) + L_o \frac{d}{dt} (i_r e^{j \, \cot})$$

$$= R_s i_s e^{j \, \cot} + L_s \frac{di_s}{dt} + j \, \omega L_s i_s e^{j \, \cot} + L_o \frac{di_r}{dt} e^{j \, \cot} + j \, \omega L_o i_r e^{j \, \cot}.$$

Dividing by $e^{j\alpha x}$

$$u_{s} = R_{s} i_{s} + L_{s} \frac{di_{s}}{dt} + jwL_{s}i_{s} + L_{o} \frac{di_{r}}{dt} + jwL_{o}i_{r} . \tag{42}$$

From equation (4) we get

$$0 = R_r i_r e^{j \omega_r t} + L_r \frac{d}{dt} (i_r e^{j \omega_r t}) + L_o \frac{d}{dt} (i_s e^{j \omega_r t})$$

$$= R_r i_r e^{j \omega_r t} + L_r \frac{di_r}{dt} e^{j \omega_r t} + j \omega_s i_r L_r e^{j \omega_r t} + L_o \frac{di_s}{dt} e^{j \omega_r t} + j \omega_s L_o i_s e^{j \omega_r t}.$$

Dividing by $e^{j \omega_s t}$ and arranging yields

$$0 = L_o \frac{di_s}{dt} + j \omega_s L_o i_s + R_r i_r + L_r \frac{di_r}{dt} + j \omega_s L_r i_r.$$
 (43)

Where

$$i_{s} = i_{sd} + ji_{sq} ,$$

$$i_{r} = i_{rd} + ji_{rq} ,$$

$$\underline{u}_{s}(t) = u_{s}e^{j \cdot \omega t} ,$$

$$\underline{i}_{s}(t) = i_{s}e^{j \cdot \omega t} ,$$

$$\underline{i}_{r}(t) = i_{r}e^{j \cdot \omega_{r}t} ,$$

$$\varepsilon = \omega_{r}t ,$$

and

 $\omega_{x}(\omega - \omega_{x})$ is a slip angular frequency.

From (43) we get

$$L_{o} \frac{di_{s}}{dt} + L_{r} \frac{di_{r}}{dt} = -R_{r} i_{r} - j \omega_{s} L_{o} i_{s} - j \omega_{s} L_{r} i_{r}$$

$$= \frac{R_{r}}{L_{r}} L_{o} i_{s} - (\frac{R_{r}}{L_{r}} + j \omega_{s}) (L_{o} i_{s} + L_{r} i_{r}) . \tag{44}$$

Since

$$\phi_r = L_o i_s + L_r i_r , \qquad (45)$$

equation (44) can be expressed as

$$\frac{d}{dt}\phi_r = \frac{R_r}{L_r} L_o i_s - (\frac{R_r}{L_r} + j \omega_s) \phi_r . \tag{46}$$

Substituting (45) and (46) in (42) and arranging yields

$$(L_s - \frac{{L_o}^2}{L_r}) \frac{di_s}{dt} = [-(R_s + \frac{{L_o}^2}{{L_r}^2} R_r) - j \omega (L_s - \frac{{L_o}^2}{L_r})]i_s$$

$$+ \left[\frac{L_o}{L_r^2} R_r - \frac{L_o}{L_r} j \left(\omega - \omega_s \right) \right] \phi_r + u_s .$$

So,

$$L' \frac{di_s}{dt} = [-(R_s + R_r') - j\omega L'] i_s + (\frac{R_r'}{L_o} - j\omega_r \frac{L_o}{L_r}) \phi_r + u_s$$
 (47)

where

$$R_r' = \frac{L_o^2}{L_r^2} R_r ,$$

$$\omega_r = \omega - \omega_s$$
,

and

$$L' = L_s - \frac{{L_o}^2}{L_r} .$$

The reference for the inverter output voltage is calculated from (48), assuming that the stator voltage components u_{sd} and u_{sq} are controlled proportionally to the respective reference u_{sd}^* and u_{sq}^* by the PWM inverter.

$$u_{sd} = u_{sd}^* = R_s i_{sd} - \omega L' i_{sq} + \Delta V$$
 (48)

But u_{sd} can be calculated as the real part of (47)

$$u_{sd} = (R_s + R_r')i_{sd} - \omega L'i_{sq} - \frac{R_r'}{L_o} \phi_{rd} - \omega_r \frac{L_o}{L_r} \phi_{rq} + L' \frac{di_{sd}}{dt}.$$
 (49)

Since the output of the flux controller, i_{sd} , is kept constant with some gain, $L' \frac{di_{sd}}{dt}$ in (49) is relatively small compared to other terms and can be neglected while $\phi_{rd} = L_o i_{sd}$. Equation (49) then becomes

$$u_{sd} = R_s i_{sd} - \omega L' i_{sq} - \omega_r \frac{L_o}{L_r} \phi_{rq} . \qquad (50)$$

Comparing (48) with (50) gives

$$\Delta V = -\omega_r \frac{L_o}{L_r} \, \phi_{rq} \, . \tag{51}$$

Equation (51) means that ϕ_{rq} can be estimated from ΔV to which it is proportional. Furthermore, since ϕ_{rq} must be zero, ΔV need only to be zero.

$5.2 \phi_{rq}$ Zero Control

Taking (46) into consideration, the sign of ϕ_{rq} varies as shown by equation of (51) and (52).

From (46) we get

$$L_o i_{sq} - \phi_{rq} - T_r \omega_s \phi_{rd} = 0 ,$$

$$\phi_{rq} = L_o i_{sq} - T_r \omega_s \phi_{rd} .$$

where

$$T_r = \frac{L_r}{R_r} \ .$$

So,

$$\phi_{rq} \ge 0 \quad \text{when} \quad \frac{\omega_s}{i_{sq}} \le \frac{L_o}{T_r \, \phi_{rd}} \,,$$
(52)

$$\phi_{rq} < 0$$
 when $\frac{\omega_s}{i_{sq}} > \frac{L_o}{T_r \phi_{rd}}$. (53)

Therefore, it is possible to keep the flux ϕ_{rq} zero by controlling the value of $\frac{\omega_s}{i_{sq}}$, through ΔV . In practice, this could be done controlling i_{sq} (equivalent to u_{sq}) or ω_s (equivalent to ω).

The method in detail (see Figure 8) is as follows:

If $(\frac{\omega_s}{i_{sq}} - \frac{L_o}{T_r \phi_{rd}})$ is zero, no Δu_{sq} will be fed back to u_{sq}^* and if $(\frac{\omega_s}{i_{sq}} - \frac{L_o}{T_r \phi_{rd}})$ is not zero, Δu_{sq} , the difference between $\frac{\omega_s}{i_{sq}}$ and $\frac{L_o}{T_r \phi_{rd}}$, will be fed back to u_{sq}^* .

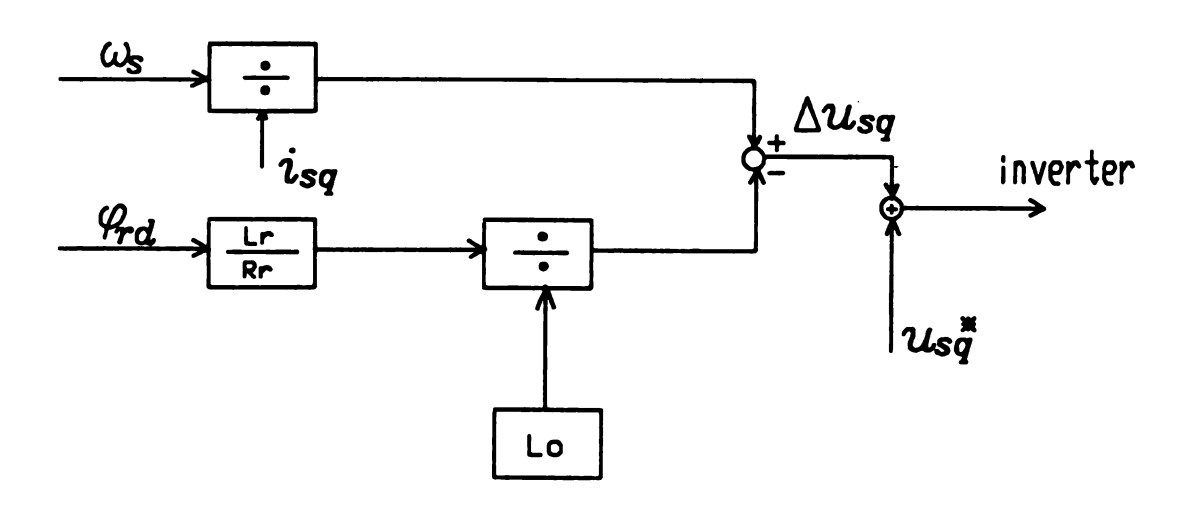


Figure 8. Compensation for flux deviation.

CHAPTER VI

FLUX POSITION CONTROLLER AND COORDINATE TRANSFORMATION

6.1 Flux Position Controller

Since we have analyzed the control scheme in d-q coordinates, we have to control the rotor flux position. The position of the voltage components in the stationary reference frame to establish the demanded field components is quite important.

The acceleration or deceleration of the flux vector depends on the slip reference (demanded slip) and actual slip calculated from (34). The slip reference is calculated from (14), repeated here for convenience.

$$\omega_s^* = \frac{i_{sq}^*}{T_r i_{mr}^*} \tag{14}$$

The slip error quantity $\omega_s^* - \omega_s$ is the error in the angular speed at any instant required for the flux vector to attain the desired position. The integral of the error quantity gives the required displacement of the flux vector.

This is done by the flux position controller, which is basically a PI controller with small gain. The output of the controller gives $\Delta \rho$, the increment of ρ . The desired position of the flux vector ρ_o is then given by $\rho_o = \rho + \Delta \rho$ and a diagram is shown in Figure 9.

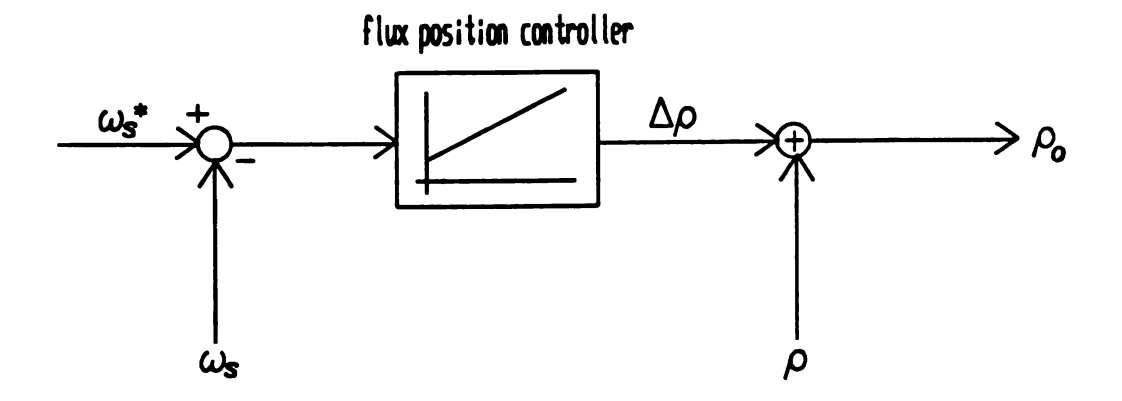


Figure 9. A diagram of flux position controller.

6.2 Coordinate Transformation

From the d and q-axis components of the stator voltage and using the following inverse coordinate transformation, the voltage components are obtained as

$$\begin{bmatrix} V_{s\alpha} \\ V_{s\beta} \end{bmatrix} = \begin{bmatrix} \cos \rho_o & -\sin \rho_o \\ \sin \rho_o & \cos \rho_o \end{bmatrix} \begin{bmatrix} V_{sd} \\ V_{sq} \end{bmatrix}. \tag{54}$$

The three phase quantities are obtained from $V_{s\alpha}$, $V_{s\beta}$ by 2-axis to 3-axis transformation as

$$\begin{bmatrix} V_{s1} \\ V_{s2} \\ V_{s3} \end{bmatrix} = \begin{bmatrix} \frac{1}{-1} & \frac{0}{\sqrt{3}} \\ \frac{-1}{2} & \frac{-\sqrt{3}}{2} \\ \end{bmatrix} \begin{bmatrix} V_{s\alpha} \\ V_{s\beta} \end{bmatrix}.$$
 (55)

These three phase quantites serve as the reference voltage to the inverter. The inverter was modeled as a small delay element, which can be ignored considering the whole dynamic response of the system. Hence, the reference voltage serves as the input to the motor.

For the 2-axis model of the motor, the three phase quantities are converted to two phase quantities through the following transformation as

$$\begin{bmatrix} V_{s\alpha} \\ V_{s\beta} \end{bmatrix} = \begin{bmatrix} 1 & 0 & 0 \\ 0 & \frac{1}{\sqrt{3}} & \frac{-1}{\sqrt{3}} \end{bmatrix} \begin{bmatrix} V_{s1} \\ V_{s2} \\ V_{s3} \end{bmatrix}.$$
 (56)

CHAPTER VII

PI Controller

The controllers used in this scheme are the proportional and integral(PI) type. The equation of a continuous PI controller is written as

$$H(s) = \frac{Y(s)}{E(s)} = K_c \left(1 + \frac{1}{\tau s}\right)$$

$$= K_c \left(1 + \frac{1}{\tau} s^{-1}\right). \tag{57}$$

where

τ is the time constant,

and

 K_c is the gain.

Using the simple rectangular approximation for s^{-1} with T_s as a sampling time, we get

$$H(z) = \frac{Y(z)}{E(z)} = K_c \left(1 - \frac{1}{\tau} \frac{T_s}{1 - z^{-1}}\right)$$

$$= K_c \frac{1 - z^{-1} + \frac{T_s}{\tau}}{1 - z^{-1}}$$

$$= K_c \left(\frac{z \left(1 + \frac{T_s}{\tau}\right) - 1}{z - 1}\right)$$

$$= \frac{K_c}{\frac{\tau}{(\tau + T_s)}} \frac{\frac{z - \tau}{(\tau + T_s)}}{z - 1}.$$
 (58)

where

$$s=\frac{1-z^{-1}}{T_s}.$$

Then,

$$H(z) = \frac{K_c}{\alpha} \frac{z - \alpha}{z - 1} . ag{59}$$

where -

$$\alpha = \frac{\tau}{\tau + T_s}.$$

So,

$$Y(z)(z-1) = \frac{K_c}{\alpha}(z-\alpha)E(z). \tag{60}$$

Taking inverse z transform yields

$$y(n) = y(n-1) + \frac{K_c}{\alpha} e(n) - K_c e(n-1).$$
 (61)

CHAPTER VIII GATE PULSE GENERATION

8.1 Pulse Width Modulation for 3-Phase Inverter

The generation of the gate pulse signals can be divided into two parts.

One is to determine the firing time of each transistor and the other is to generate the gate pulse at some determined time.

The PWM signal is generated as a three-phase square signal as shown in Figure 10, by comparing a three-phase sine wave signal (modulation signal) to a triangular wave signal (carrier signal).

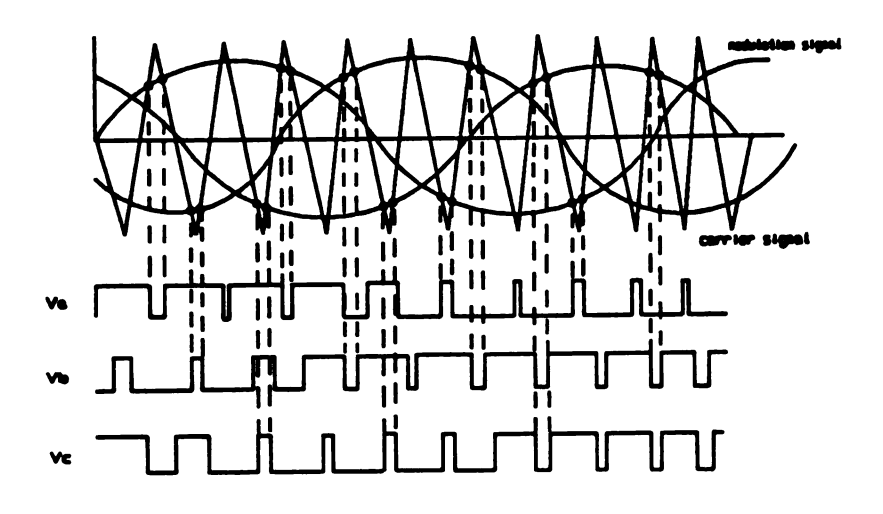


Figure 10. The principle of PWM signal generation.

8.2 Generation of Pulses from Frequency, Magnitude and Phase Angle

The modulation signal corresponds to the reference values of the voltage frequency f, magnitude u_s , and phase angle $\Delta \rho$. The width of the square signal changes at each crossing point. This relation is

$$u_s = \sqrt{(u_{sq}^*)^2 + (u_{sd}^*)^2}$$

and

$$\Delta \rho = \tan^{-1} \frac{u_{sq}^*}{u_{sd}^*} .$$

When a microprocessor is used for the generation of the firing pulse, it reads the values of ρ, u_s and $\Delta \rho$ from memory at the controller [7]. The instantaneous form of the modulation signal V_a is expressed as

$$V_a = u_s \sin(\rho + \Delta \rho).$$

The power converter performs a switching operation in response to the gate pulse signals.

Consider the three-phase bridge inverter in shown Figure 11. It has three parallel branches, each corresponding to one output phase and consisting of two fully controlled semiconductor power switches and two freewheeling diodes. At any instant time, one of the switches in each branch must be ON while the other must be OFF [8]. By this condition, we can define logic states as follows:

if Si is OFF and Si' is ON, the logic state of this branch is 0 for i=A, B, C.

The logic state of the whole inverter can be designated by a three bit binary number abc. For example, logic state 6 corresponds to $(abc)_6 = 110$, i.e., thyristor SA, SB and SC' are in ON and SA', SB', and SC are in OFF.

The line to neutral and line to line voltages of the inverter can be expressed in terms of the logic variables and supply voltage E_d as

$$V_{XN} = \frac{E_d}{3} (2x - y - z) \tag{62}$$

and

$$V_{XY} = E_d (x - y) \tag{63}$$

where X and Y denote any two of A, B and C phases and x, y and z is a corresponding sequence of a, b and c logic variables. For example, a = 1, b = 1 and c = 0 in the case $(abc)_6$.

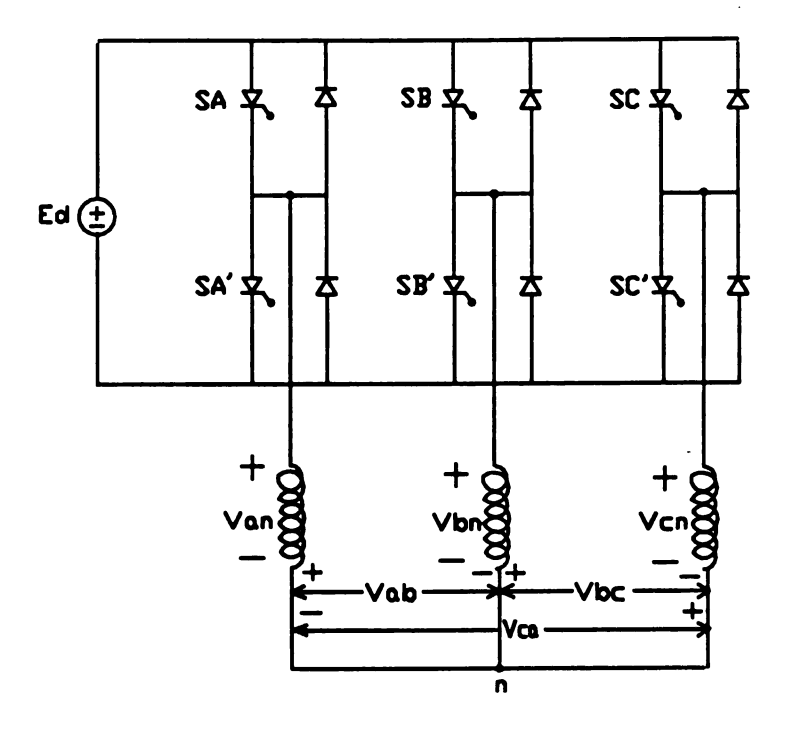


Figure 11. Three phase bridge inverter.

8.3 Harmonics Due to PWM

The PWM signals $a(\omega r)$, $b(\omega r)$ and $c(\omega r)$ of the switching function as well as the corresponding sequence of logic states of the inverter are shown in Figure 12. The 2π output voltage period is divided into N equal switching intervals $\Delta \alpha$. The central angle of nth switching interval is designated by α_n . The switching angles are denoted by α_{1n} for switch ON angles and α_{2n} for switch OFF angles. Duration of individual logic states are designated by Δ_j .

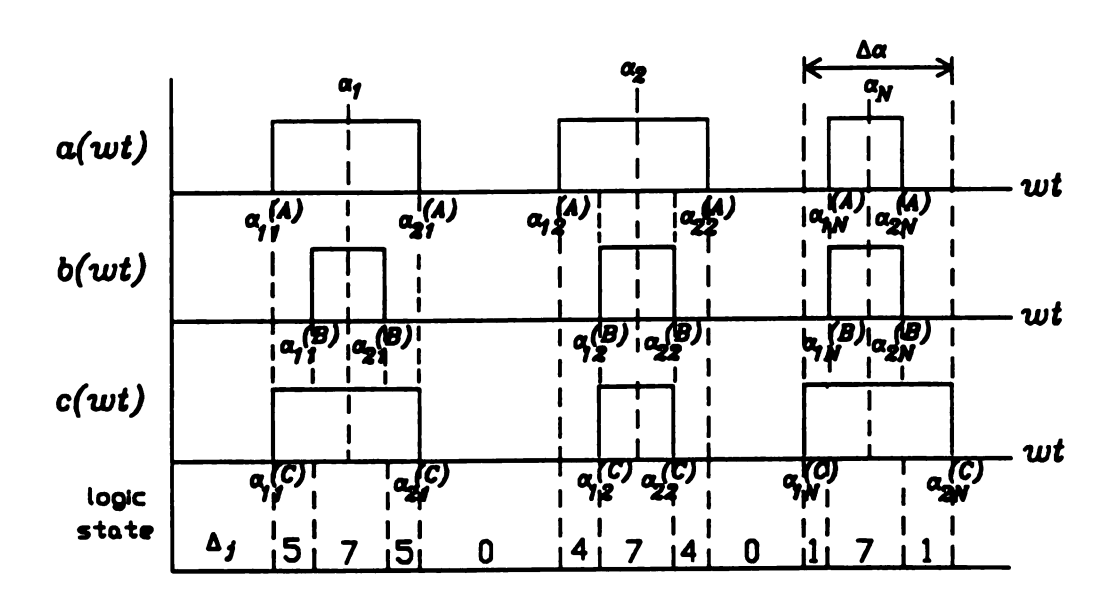


Figure 12. Switching function of a PWM inverter.

The ratio of a switching function pulse width to the switching interval is referred to as switching ratio given by

$$\gamma^{(X)}(\omega \mathbf{r}) = \gamma_n^{(X)} = \frac{\alpha_{2,n}^{(X)} - \alpha_{1,n}^{(X)}}{\Delta \alpha}$$
for $\alpha_n - \frac{\Delta \alpha}{2} \le \omega \mathbf{r} \le \alpha_n + \frac{\Delta \alpha}{2}$. (64)

Since a close relationship between the harmonic spectrum of $\gamma^{(X)}$ and that of inverter output voltage can be expected, a strong adjustable fundamental of $\gamma^{(X)}(\omega r)$ is desirable.

Obviously, the switching ratio can only assume values between 0 and 1. Hence, the simplest switching function is as follows and is shown to Figure 13.

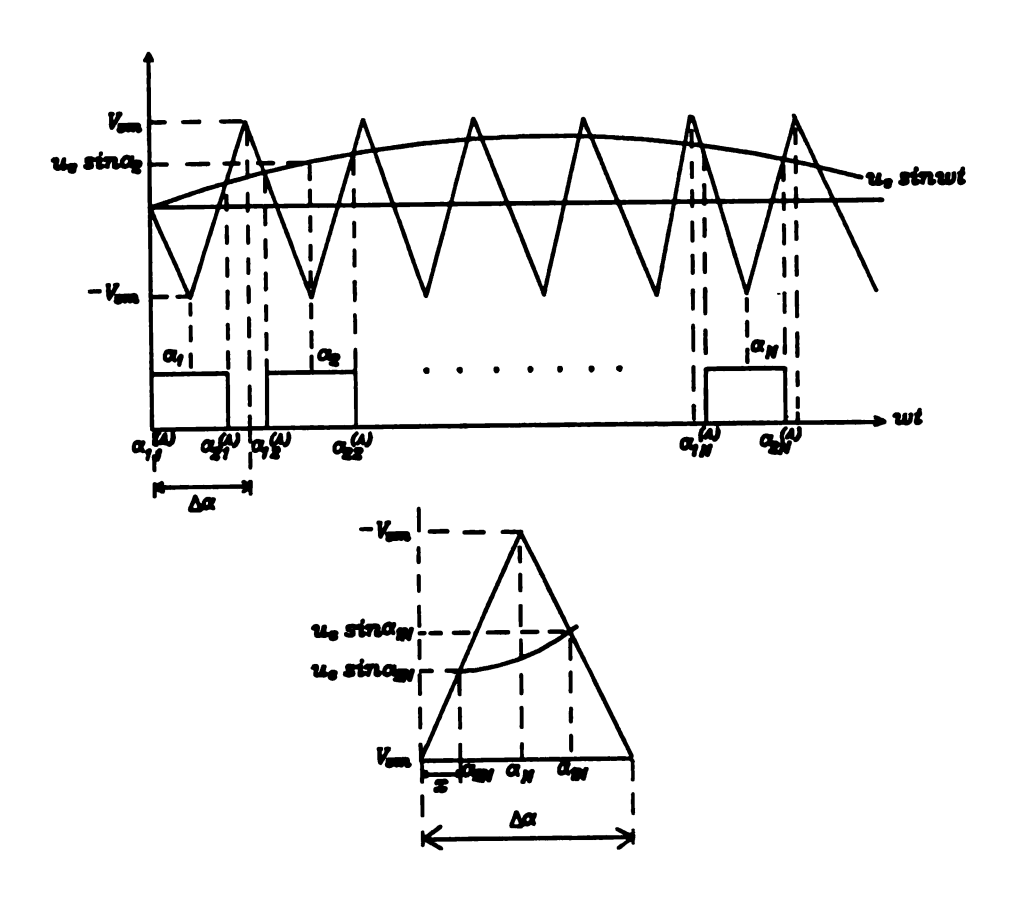


Figure 13. PWM configuration.

$$\frac{2V_{sm}}{\frac{\Delta\alpha}{2}} = \frac{V_{sm} - u_s \sin\alpha_{2n}}{x}$$

$$=\frac{V_{sm}-u_{s}\sin\alpha_{1n}}{\Delta\alpha-(x+\alpha_{2n}-\alpha_{1n})}.$$
 (65)

Hence,

$$x = \frac{\Delta \alpha}{4V_{sm}} (V_{sm} - u_s \sin \alpha_{2n}) . \tag{66}$$

Therefore,

$$\alpha_{2n} - \alpha_{1n} = \Delta \alpha - \frac{\Delta \alpha}{4V_{sm}} (V_{sm} - u_s \sin \alpha_{1n}) - x$$

$$= \frac{\Delta \alpha}{2} + \frac{\Delta \alpha}{2V_{sm}} u_s \sin \alpha_n$$
(67)

where

$$m = \frac{u_s}{V_{sm}}$$

and

$$\frac{u_s \sin \alpha_{1n} + u_s \sin \alpha_{2n}}{2} = u_s \sin \alpha_n.$$

Finally,

$$\gamma_n^{(A)} = \frac{1}{2} (1 + m \sin \alpha_n)$$
, (68)

$$\gamma_n^{(B)} = \frac{1}{2} (1 + m \sin(\alpha_n - \frac{2}{3}\pi)),$$
 (69)

and

$$\gamma_n^{(C)} = \frac{1}{2} (1 + m \sin(\alpha_n - \frac{4}{3}\pi)),$$
 (70)

where m denotes magnitude control ratio (0 < m < 1).

In practice, it is sufficient to only modulate the switching function $a(\omega r)$ according to (68) and shift the resulting pattern of switching angles by $\frac{2}{3}\pi$ and $\frac{4}{3}\pi$ to obtain $b(\omega r)$ and $c(\omega r)$, whose switching ratios satisfy (69) and (70) respectively.

Using (64), the switch-ON and switch-OFF angles can be calculated as

$$\alpha_{1,n}^{(X)} = \alpha_n - \gamma_n^{(X)} \frac{\Delta \alpha}{2} \tag{71}$$

and

$$\alpha_{2,n}^{(X)} = \alpha_n + \gamma_n^{(X)} \frac{\Delta \alpha}{2}$$
 (72)

where

$$\Delta \alpha = \frac{2\pi}{N} ,$$

$$\alpha_n = (n - \frac{1}{2}) \Delta \alpha ,$$

and

$$n = 1,2,3,...,N-1,N$$
.

We can then express $a(\omega t)$, $b(\omega t)$ and $c(\omega t)$ by using Fourier Series as

$$a(\omega r) = a_o + \sum_{k=1}^{\infty} a_k \cos k \omega r + b_k \sin k \omega r ,$$

$$a_o = \frac{1}{2\pi} \int_0^{2\pi} \gamma_n^{(A)} d\alpha$$

$$= \frac{1}{4\pi} \int_{0}^{2\pi} d\alpha + \frac{m}{4\pi} \int_{0}^{2\pi} \sin\alpha d\alpha = \frac{1}{2}, \qquad (73)$$

$$\lim_{N \to \infty} a_k = \frac{1}{\pi} \int_0^{2\pi} \gamma_n^{(A)} \cos k \alpha d\alpha$$

$$= \frac{1}{2\pi} \int_0^{2\pi} \cos k \alpha d\alpha + \frac{m}{2\pi} \int_0^{2\pi} \sin \alpha \cos k \alpha d\alpha = 0, \qquad (74)$$

$$\lim_{N \to \infty} b_k = \frac{1}{\pi} \int_0^{2\pi} \gamma_n^{(A)} \sin k \alpha d\alpha$$

$$= \frac{1}{2\pi} \int_0^{2\pi} \sin k \alpha d\alpha + \frac{m}{2\pi} \int_0^{2\pi} \sin \alpha \sin k \alpha d\alpha,$$

and

$$b_k = \begin{cases} \frac{m}{2} & \text{if } k = 1\\ 0 & \text{otherwise} \end{cases}$$
 (75)

Hence, the higher number of pulses N attenuates the lower-order harmonics of the inverter switching functions while the fundamental approaches the value of half of the control ratio m. Also, by selecting N as a multiple of 3, the triplen frequency-related currents can be avoided in the line.

If, as assumed

$$a(\omega t) = b(\omega t - \frac{2}{3}\pi) = c(\omega t - \frac{4}{3}\pi)$$

then, the per unit harmonic spectrum of line to neutral inverter voltage differs from that of the switching function.

The magnitude of the remaining voltage harmonic is equal to those of the switching function, times the supply voltage E_d . The line to line voltages have the same harmonics as the line to neutral voltage only $\sqrt{3}$ times greater in magnitude.

Hence, in the described PWM scheme, the r.m.s. values of fundamentals line to neutral and line to line voltage are

$$V_{XN(rms)} = m \frac{\sqrt{2}}{4} E_d \tag{76}$$

and

$$V_{XY(rms)} = m \frac{\sqrt{6}}{4} E_d . \tag{77}$$

Equations (76) and (77) show that the fundamental of the inverter output voltage can be linearly controlled by adjusting the control ratio m. The length of Δ_j changes with the magnitude control ratio m but the sequence of Δ_j (logic state interval) remains unvaried.

8.4 Hardware Implementation

The basic hardware configuration of the PWM signal generation circuit is shown Figure 14.

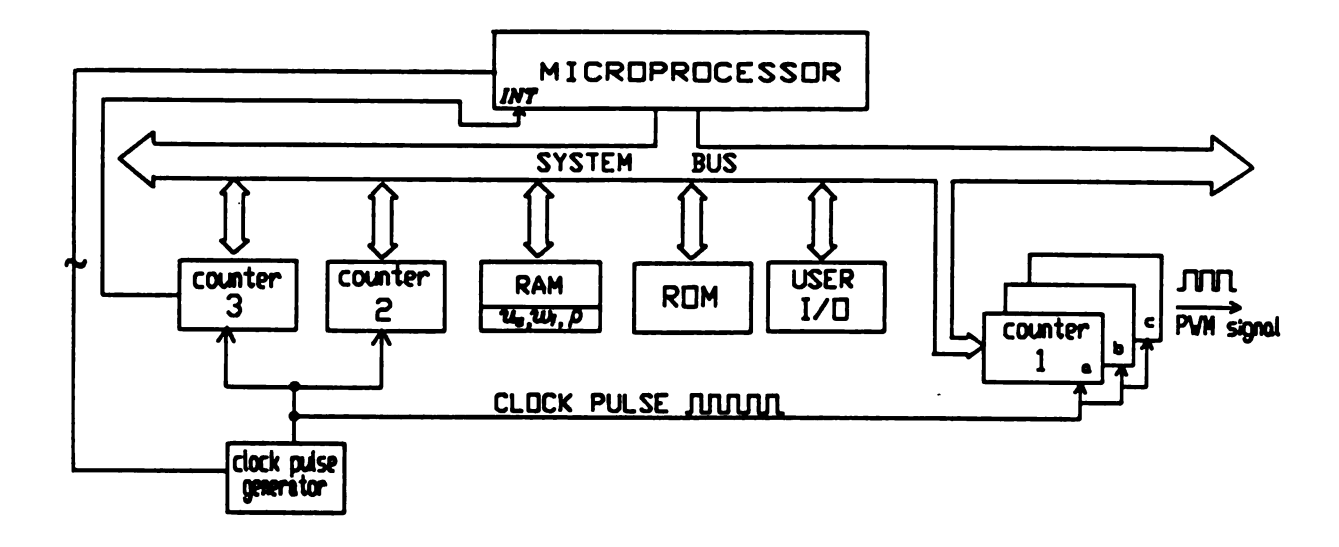


Figure 14. Hardware configuration of PWM generation.

We define time intervals of logic states as

$$\tau_j = \frac{\Delta_j}{2\pi f} \ . \tag{78}$$

Output bit signals a, b and c represent the logic variables of the inverter.

A programmable counter is used to generate a pulse of width τ_j . To produce switching functions $a(\omega t)$, $b(\omega t)$ and $c(\omega t)$ appropriate three bit numbers (abc) are loaded in the I/O device.

Counter-1 generates a pulse of width τ_j while counter-2 is being programmed for the next pulse. Counter-3, activated by the clock pulse generator, serves as frequency divider to produce the clock signal for counter-1 and counter-2.

When the interval τ_j has elapsed, the microprocessor is interrupted by the counter. The interrupt service routine sends new data to the proper counter and output device.

The microprocessor reads input f, m and ρ from common memory. If f and/or m are found to have changed, a next look-up table of logic states $(abc)_2$ and time interval τ_j is computed. Firstly, the number N of the pulses per period is determined according to an assumed N versus f relation. Secondly, time intervals calculated from (78) are assigned to successive logic states in an appropriate sequence.

Until the next look-up table is computed, the present table is used in interrupt service routine. Then, the next table replaces the present one.

The phase control is activated by a change of the reference phase angle ρ and causes the program to branch to the pertinent location in the look-up table.

CHAPTER VIIII RESULTS AND CONCLUSIONS

9.1 Simulation Results

A number of numerical experiments were conducted to evaluate the performance of the controller. The program was written in Fortran and run on a VAX 8600 computer. Also motor parameters (Table 1), the flow chart of the controller (Figure 15) and a flow chart of the main program (Figure 16) are shown.

Table1 Motor Parameters			
P_n	5 HP	f_n	60 Hz
V_n	220 V	N_n	1800 RPM
L_s	0.0704 H	L,	0.0718 H
L_o	0.0675	$\sigma_{\!\scriptscriptstyle s}$	0.0421
σ_r	0.0631	σ	0.0973
R _s	0.444Ω	R,	0.274Ω

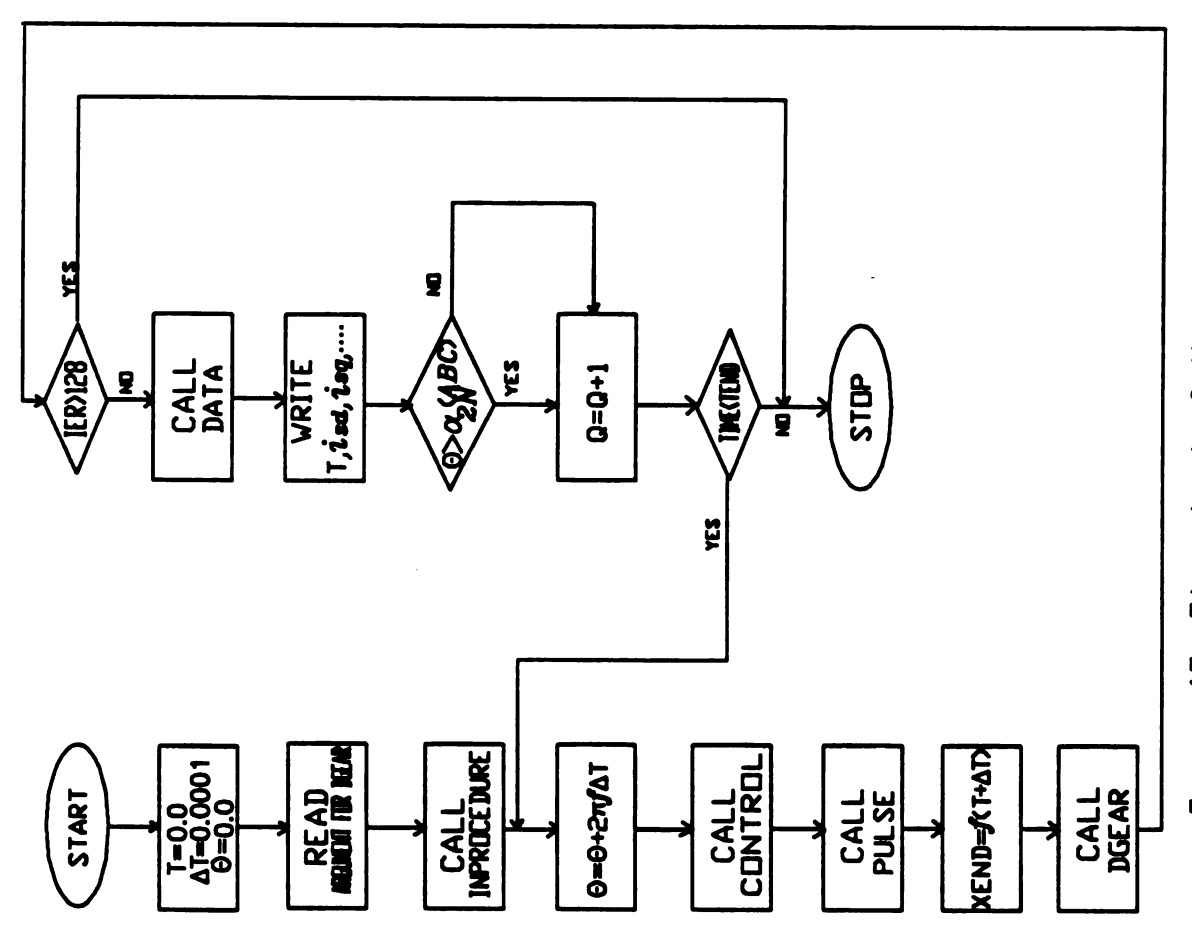


Figure 15. Flow chart of the main program

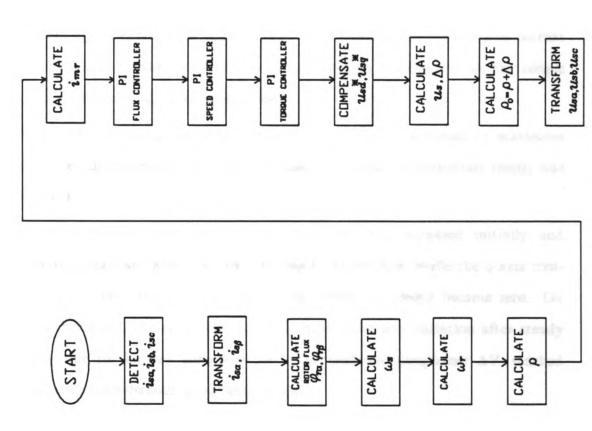


Figure 16. Flow chart of the controller

9.1.1 Acceleration Without Load

A reference speed of 377 rad/sec was given to the drive under no load condition. Fig.17-Fig.24 show the currents, speed, torque, flux and ΔV behaviour of the induction motor during running from standstill to the reference speed. The build-up of the rotor flux current i_{mr} , took 0.7 sec. The steady state value of i_{mr} was equal to the d-axis component of the stator current i_{sd} as expected in steady state, The q-component of the stator current i_{sq} remained maximum until the torque reached maximum. As the torque decreased to zero, i_{sq} also became zero.

After the flux was established, the acceleration torque increased to maximum and then decreased to zero when the reference speed (synchronous speed) was reached.

The d-axis component of the rotor flux ϕ_{rd} increased initially and remained constant after the required speed was reached, while the q-axis component of the rotor flux ϕ_{rq} reached zero when the torque became zero. On the other hand, the rotor flux ϕ_{rd} , ϕ_{rq} hardly had any variation after steady state, due to the flux compensation. The feedback component ΔV reached zero after the reference speed was reached.

It took 0.77 sec to reach reference speed and the estimated speed agrees with it. It is clear therefore that the speed control was carried out with good dynamic performance and accuracy.

From these results, it is confirmed that the torque is directly proportional to the current i_{sq} when the flux ϕ_{rq} is kept zero.

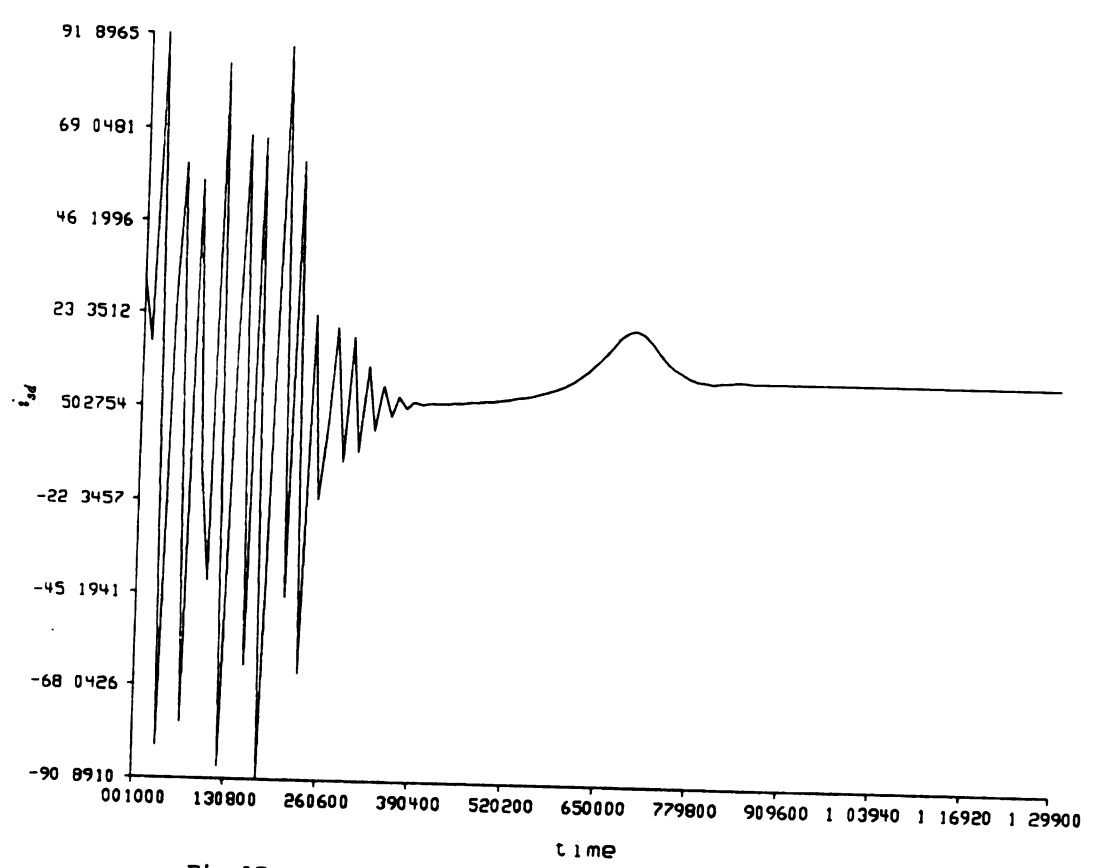


Fig.17 The d-axis stator current from standstill to 377 rad/sec

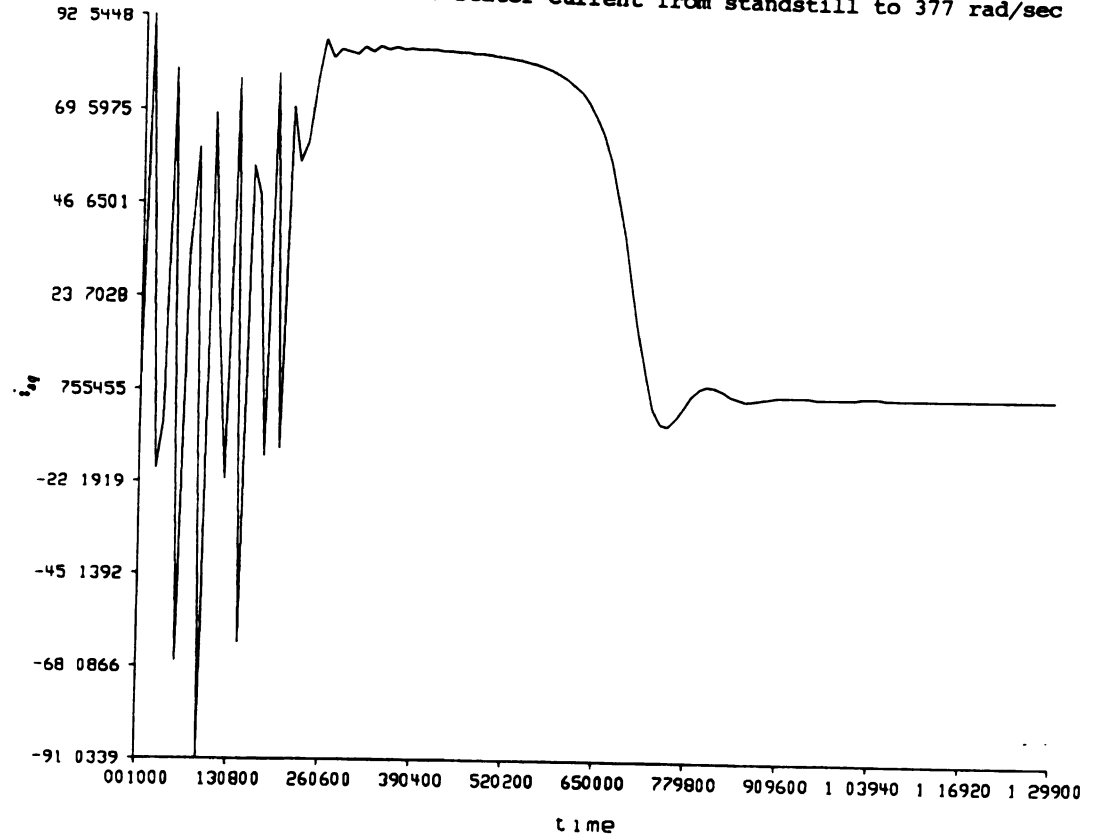


Fig.18 The q-axis stator current from standstill to 377 rad/sec

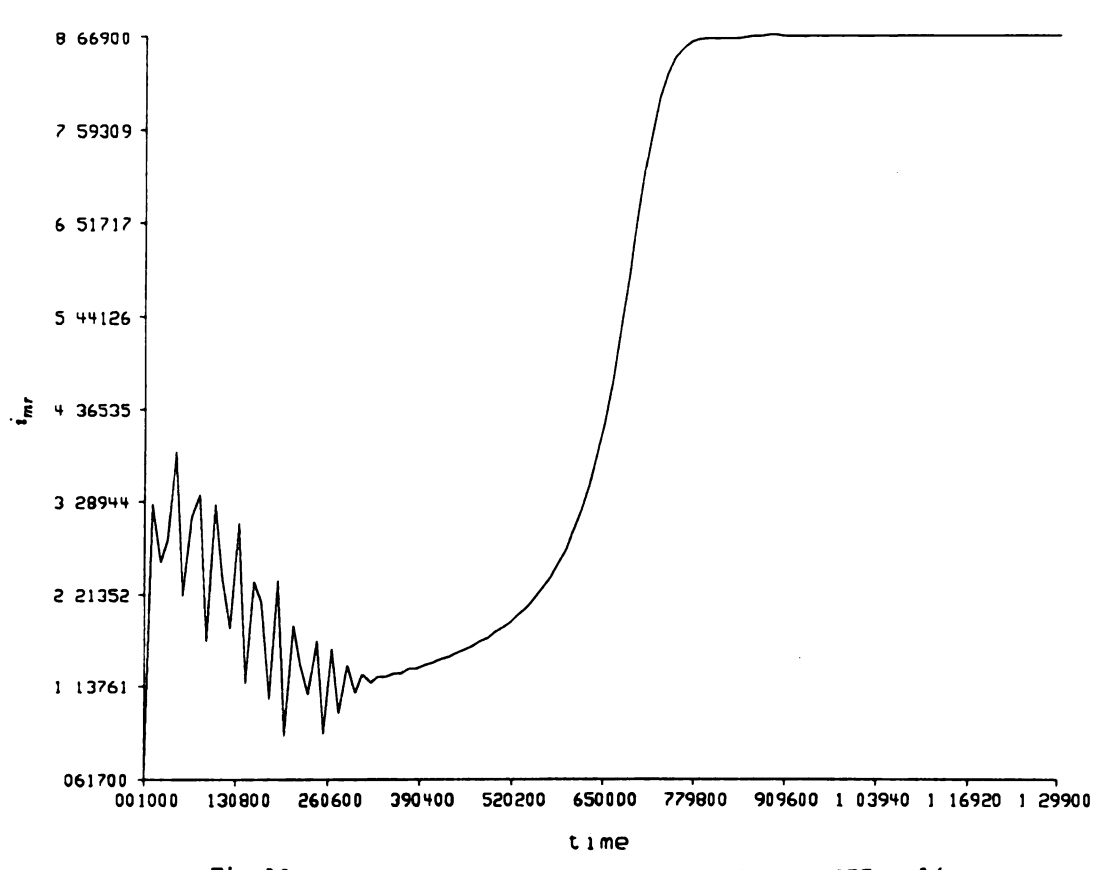


Fig.19 Rotor flux current from standstill to 377 rad/sec

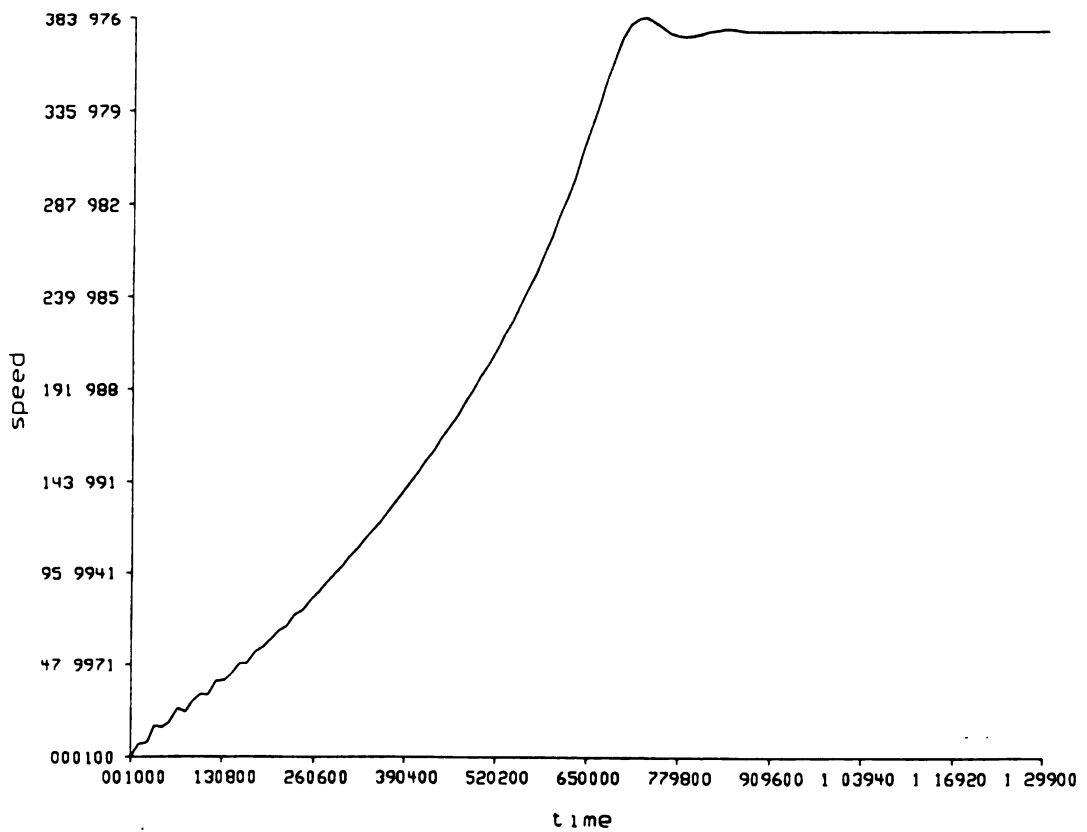
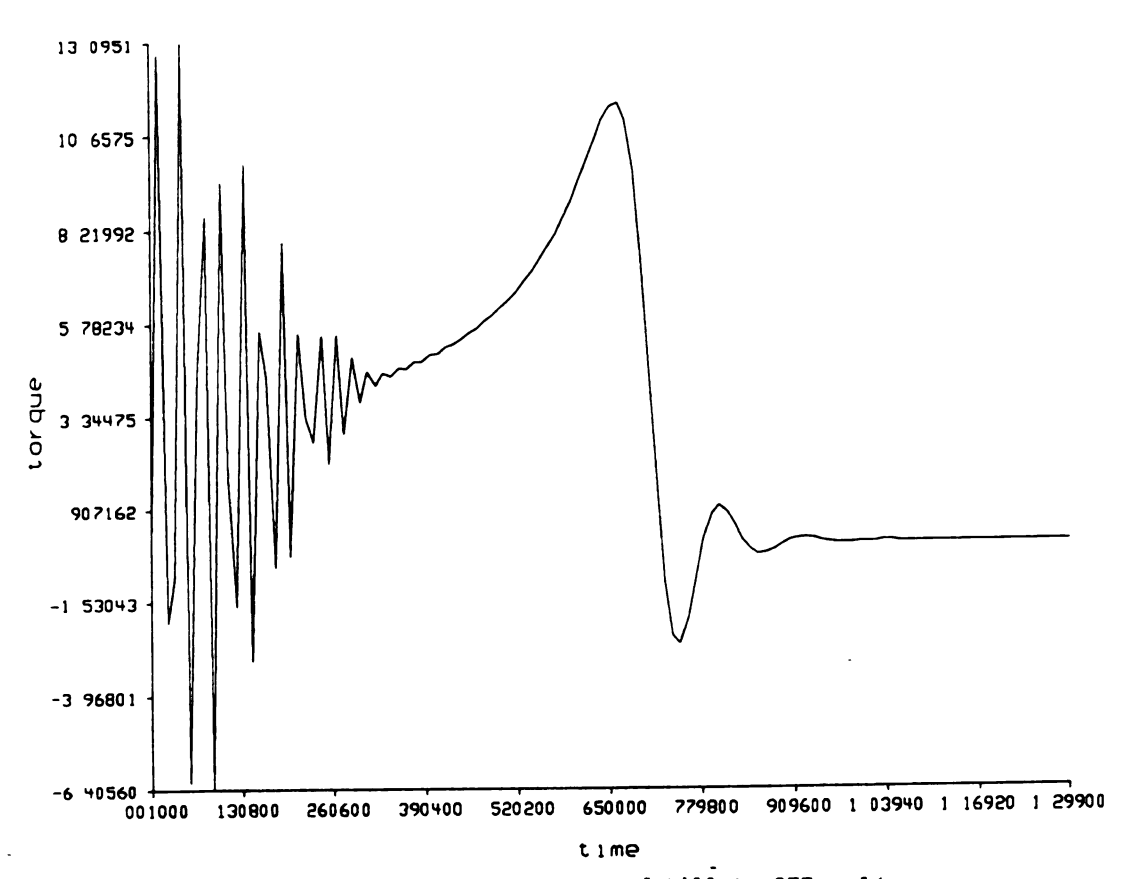
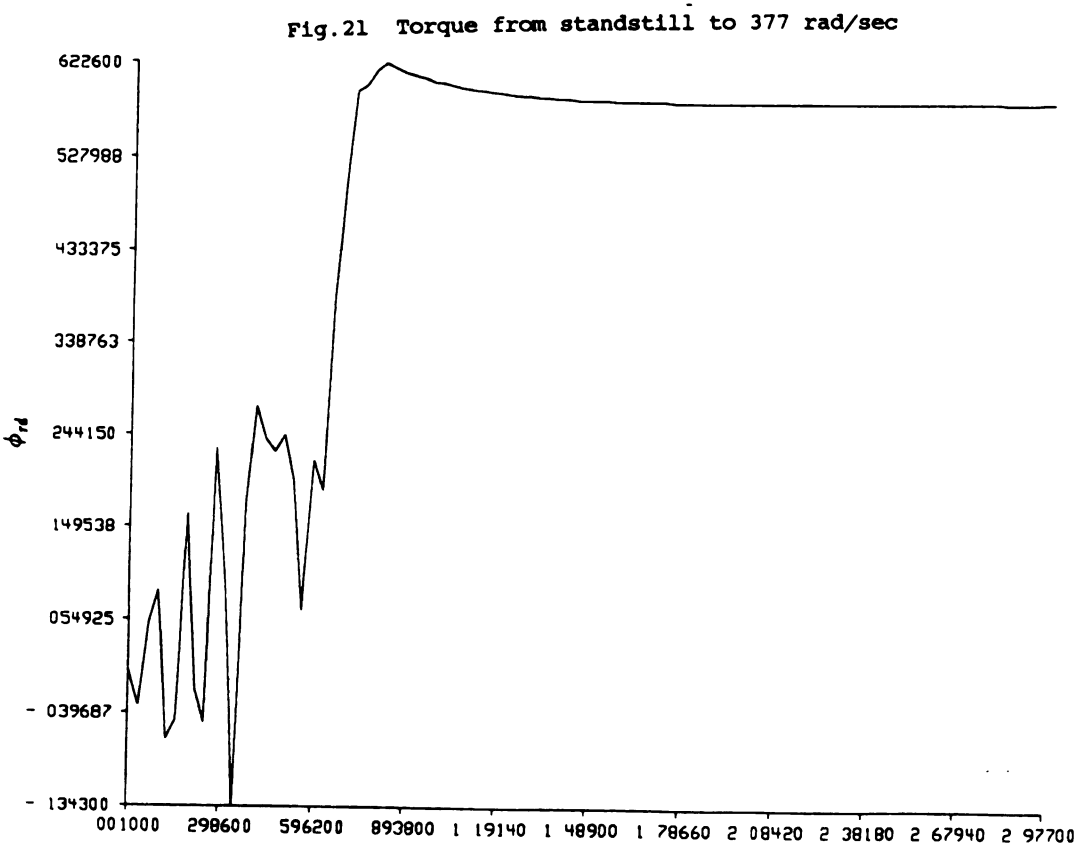
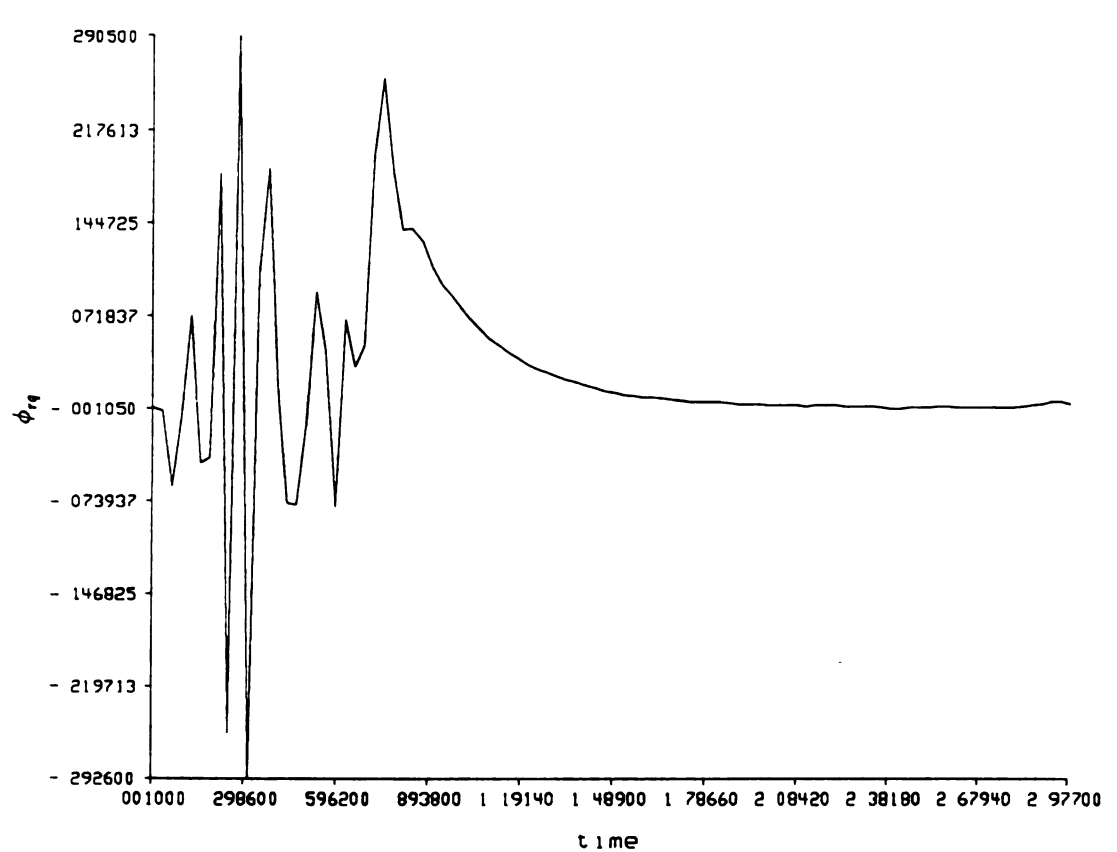


Fig. 20 Speed from standstill to 377 rad/sec





 $$t_{1}$me $$ Fig.22 The d-axis rotor flux from standstill to 377 rad/sec



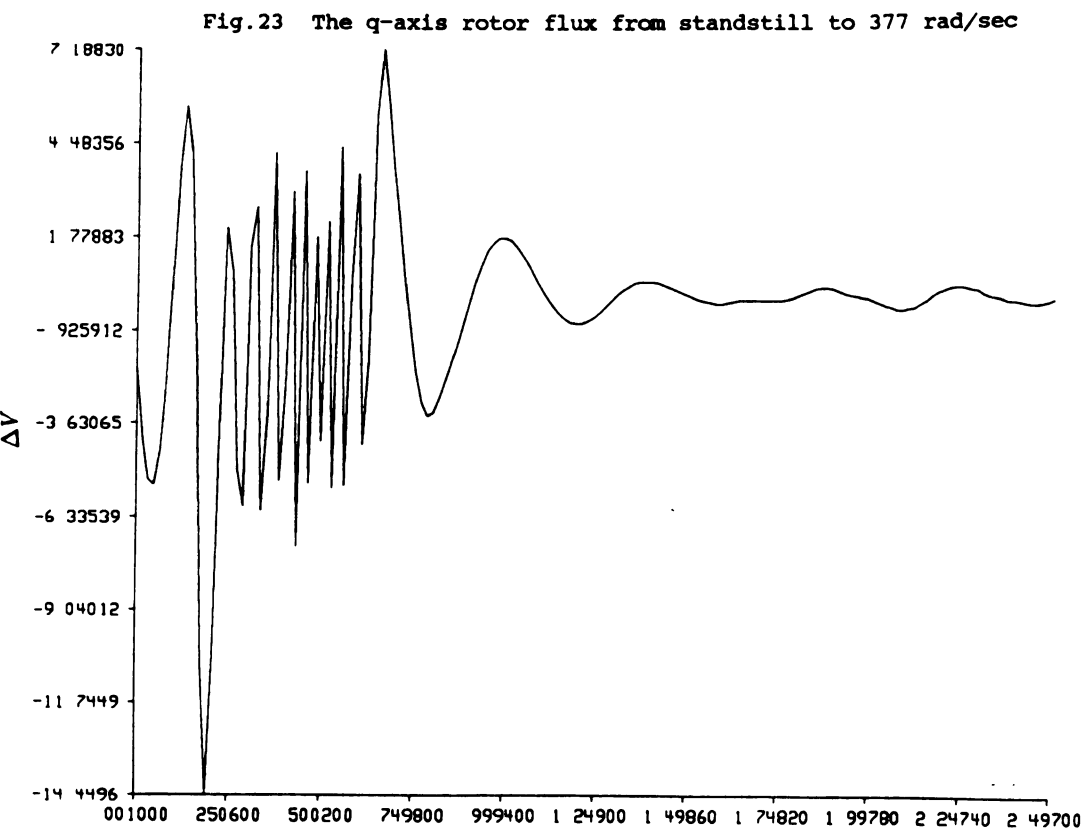


Fig. 24 Flux compensation from standstill to 377 rad/sec

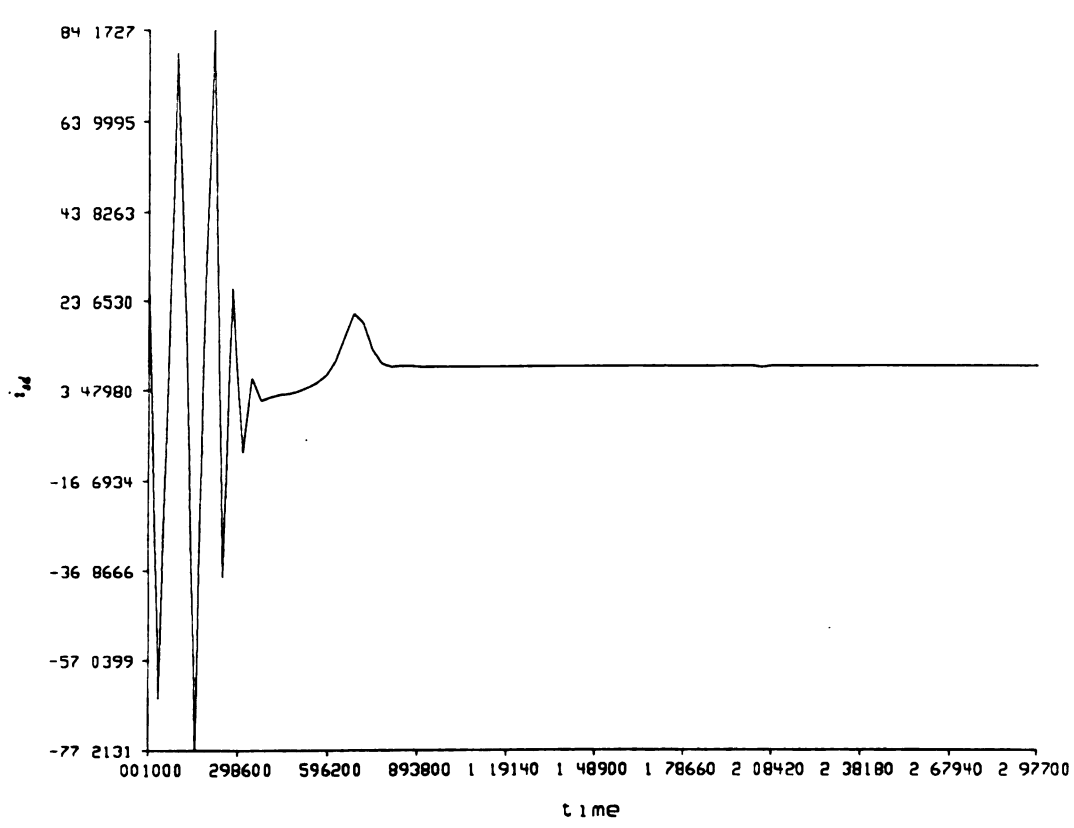
time

9.1.2 Step Load After Transient

A reference speed of 377 rad/sec was given to the drive under no load condition. After 2 sec, a step torque, equals to rated torque, was applied to the shaft. Fig.25-Fig.32 show that the currents, speed, torque, flux, ΔV responses of the motor with step torque after 2 sec. The build-up of the rotor flux current i_{mr} , took time 0.7 sec like in the the previous case. After a step torque was added, the flux remained constant. The torque was zero at synchronous speed and after the step load torque was added, it increased up to step torque quickly.

The stator current i_{sq} remained zero at synchronous speed and after the step torque was added, it quickly responded to it. During this, the current i_{sd} remained unchanged within 1 % variation. The rotor flux ϕ_{rd} , ϕ_{rq} remained unchanged within 1 % variation.

In this test, it is confirmed that this control system is stable for a quick change of the load.



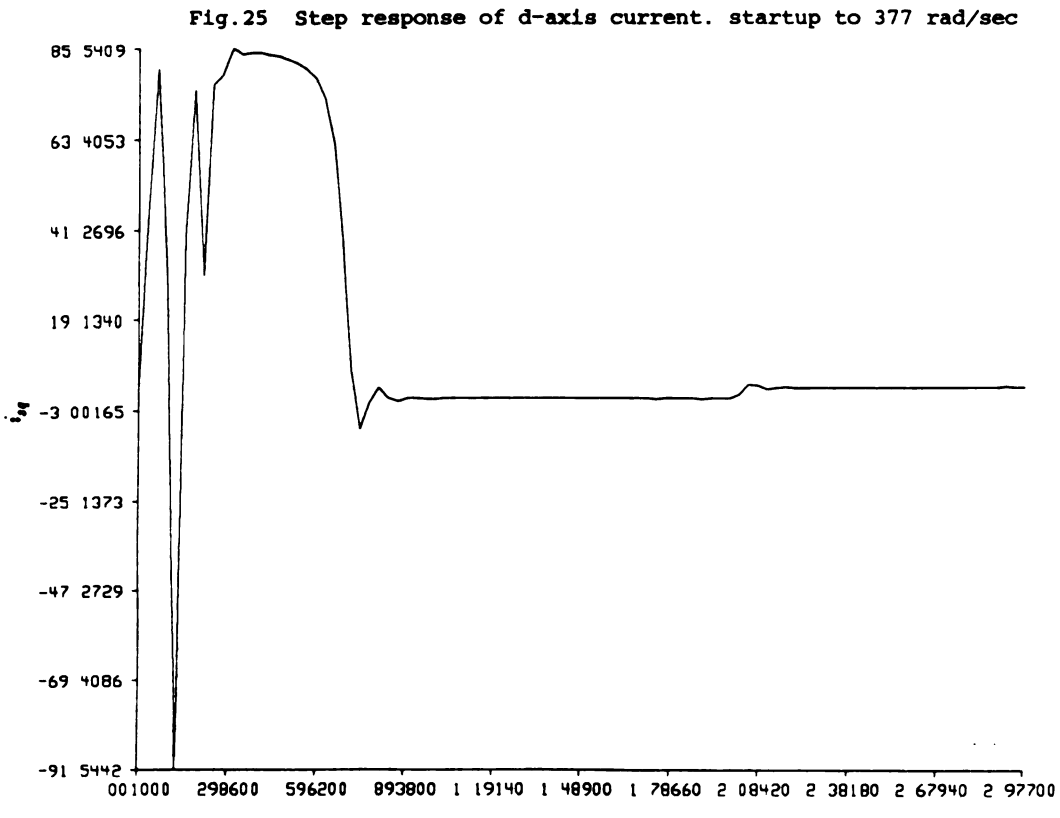


Fig. 26 Step response of q-axis current. startup to 377 rad/sec

time

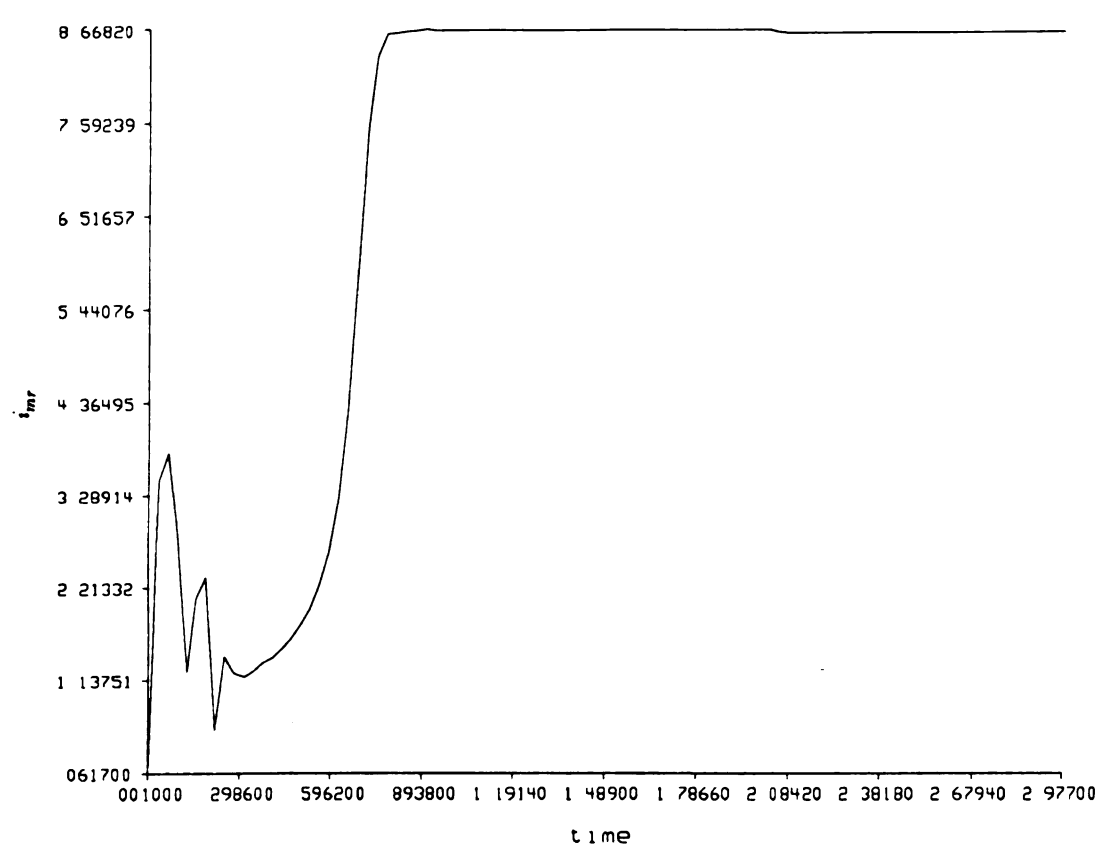


Fig. 27 Step response of rotor flux current. startup to 377 rad/sec

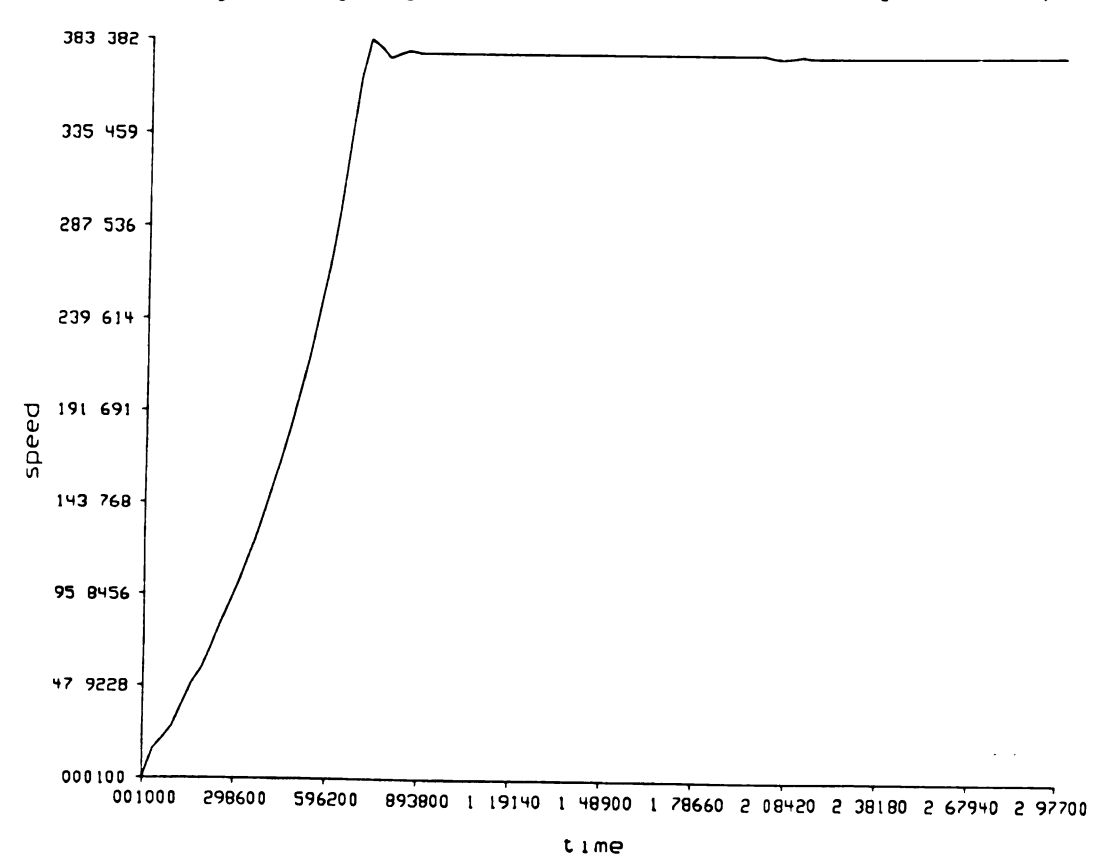


Fig.28 Step response of speed. startup to 377 rad/sec

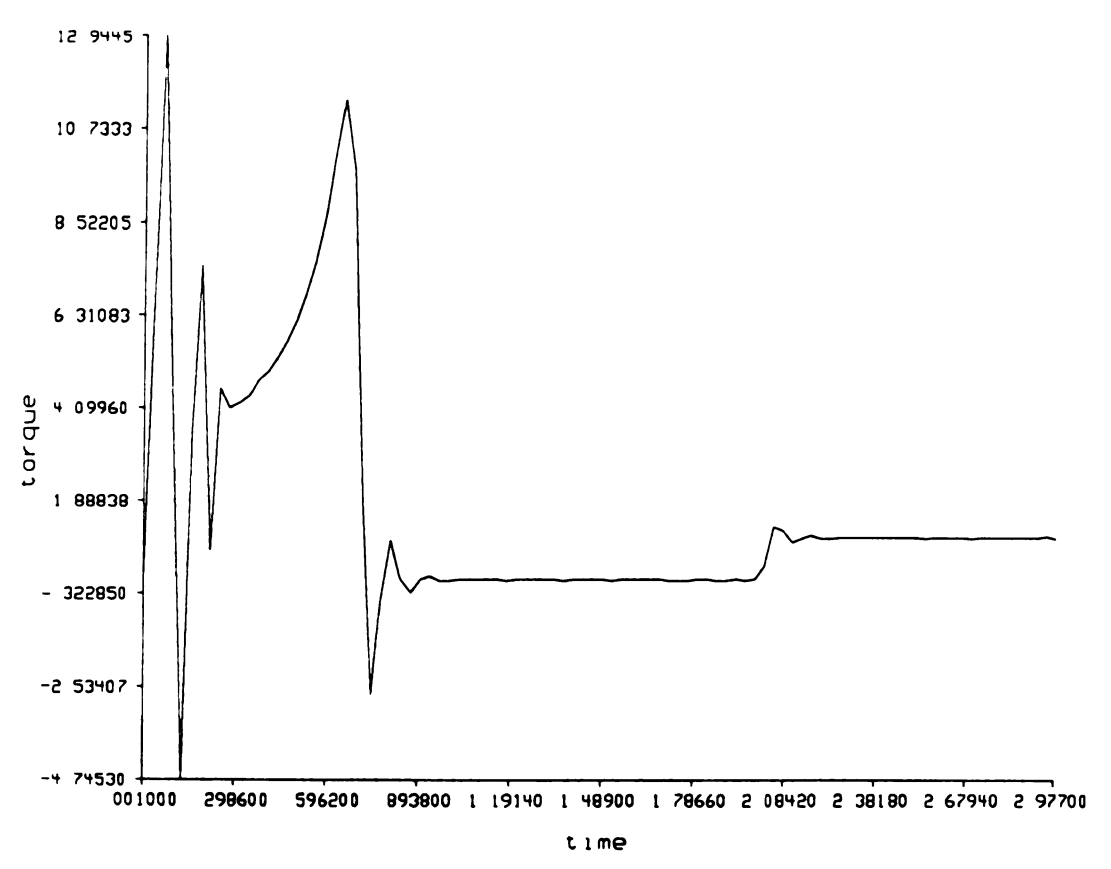


Fig.29 Step response of torque. startup to 377 rad/sec

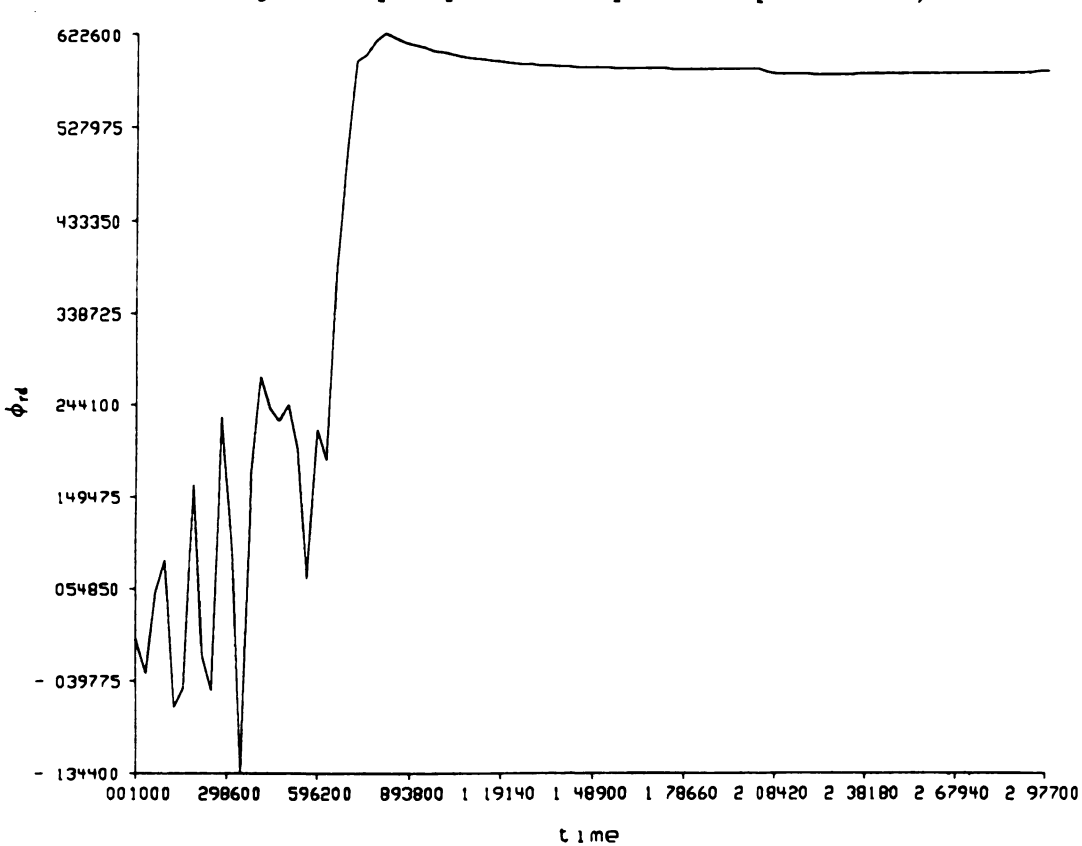


Fig.30 Step response of d-axis rotor flux. startup to 377 rad/sec

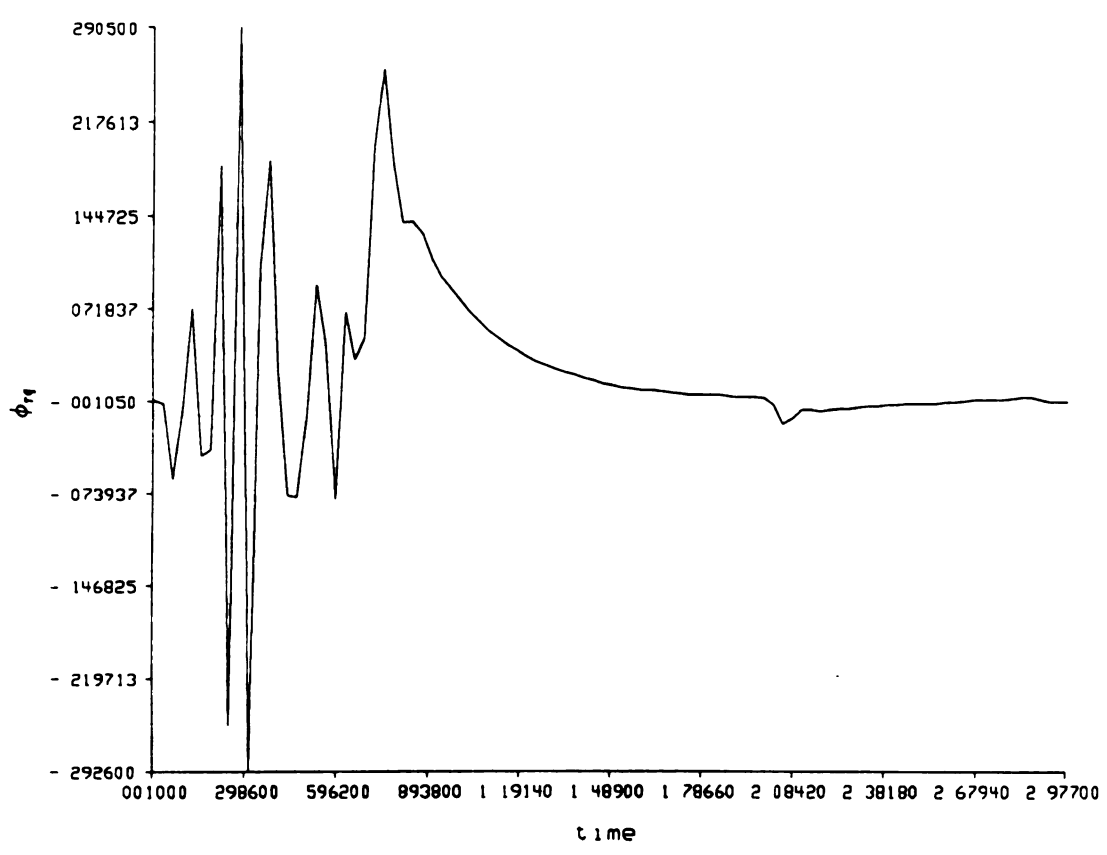


Fig.31 Step response of q-axis rotor flux. startup to 377 rad/sec

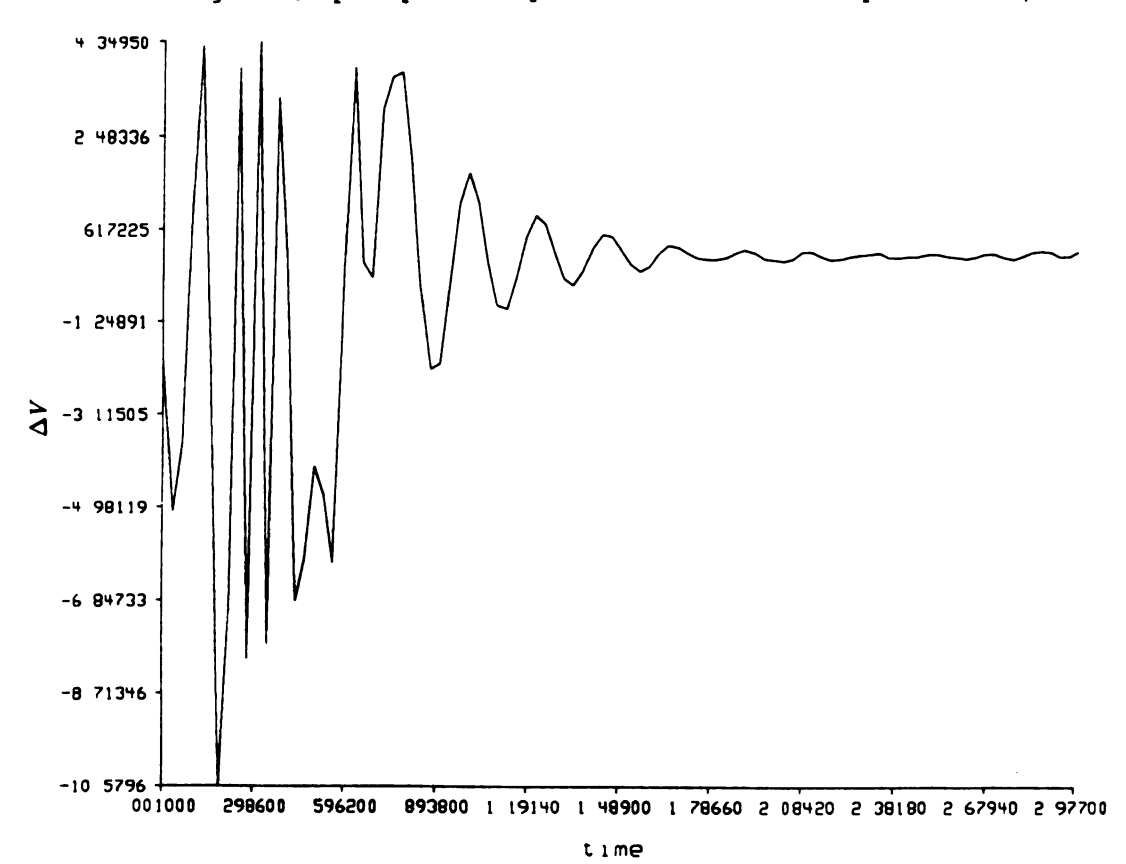


Fig. 32 Step response of flux compensation. startup to 377 rad/sec

9.1.3 Reference Speed Reversal Without Load

1.5 seconds after, reference speed of -377 rad/sec was given to the drive under no load condition. Fig.33-Fig.40 show the currents, speed, torque, flux and ΔV transient responses of the drive without load during a reversal of the reference speed.

The torque initially was zero at synchronous speed (377 rad/sec) and after the required speed was reached, it decreased to keep the speed constant and became zero again at synchronous speed (-377 rad/sec).

During the transient, the current i_{sq} remained constant(minimum) and back to zero when the required speed was reached. while the current i_{sd} remained unchanged and equal to i_{mr} at steady state (reference speed). The rotor flux ϕ_{rd} , ϕ_{rq} remained unchanged during speed reversal.

This test showed stability during the whole transient period and quick response to reference speed changes.

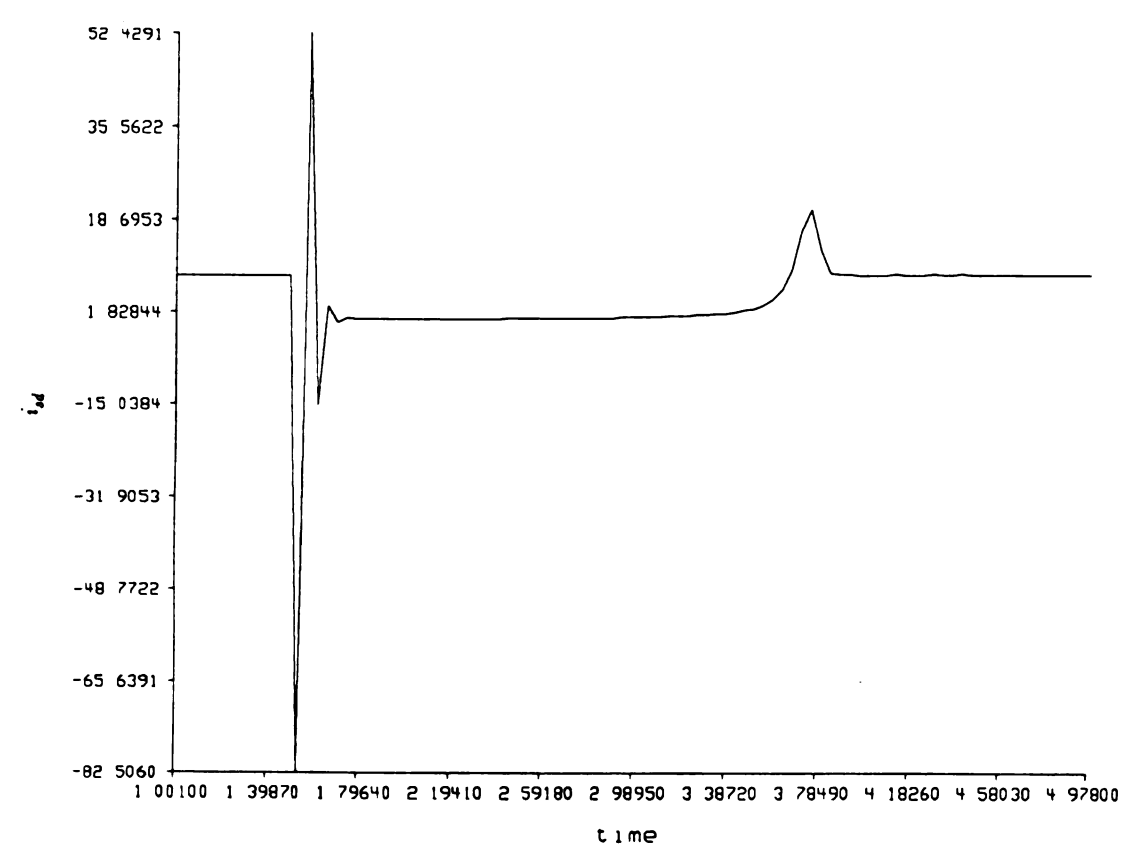


Fig.33 Speed reversal of d-axis current from 377 to -377 rad/sec

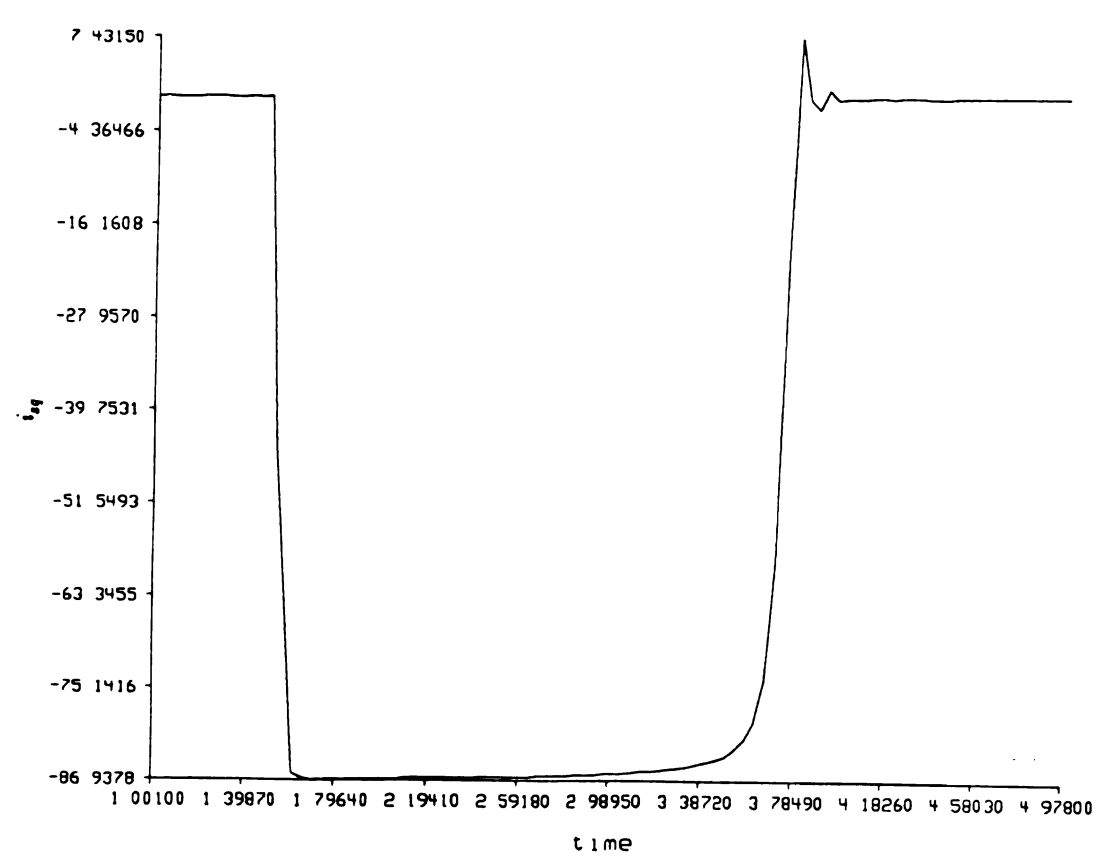


Fig.34 Speed reversal of q-axis current from 377 to -377 rad/sec

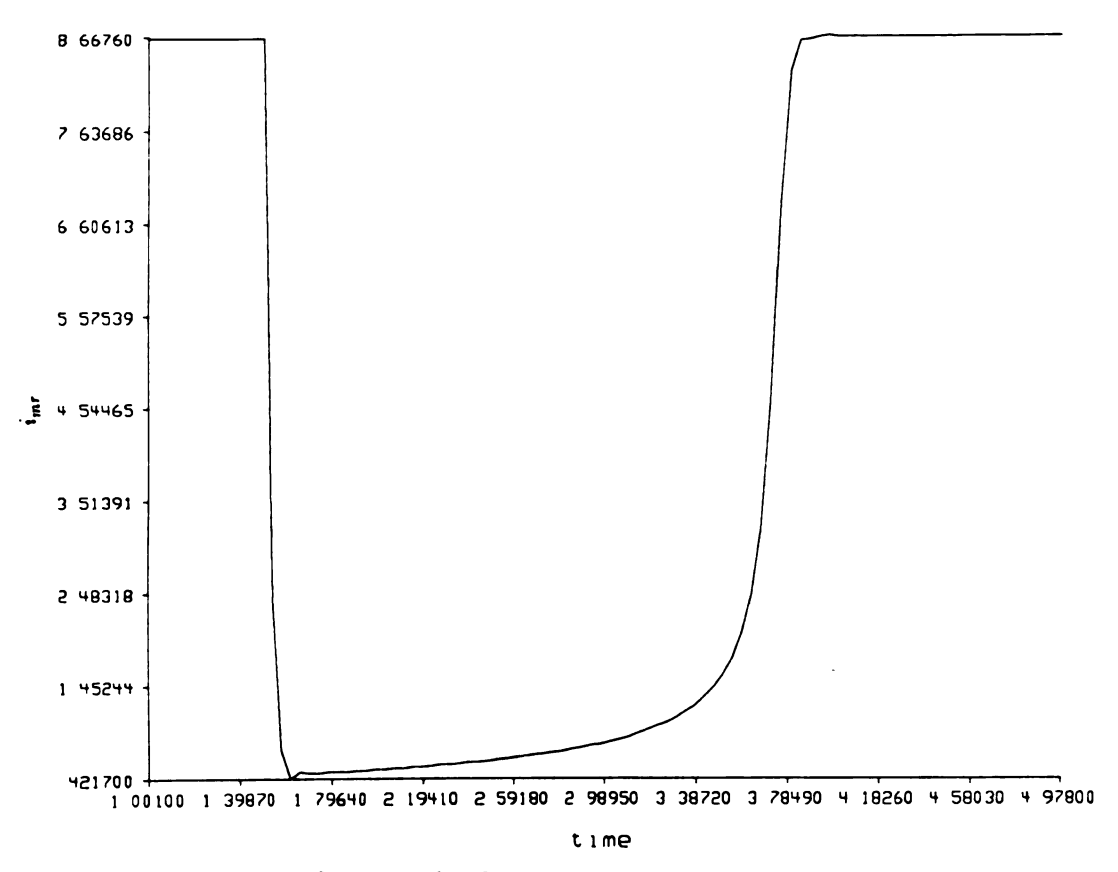


Fig.35 Speed reversal of rotor flux current from 377 to -377 rad/sec

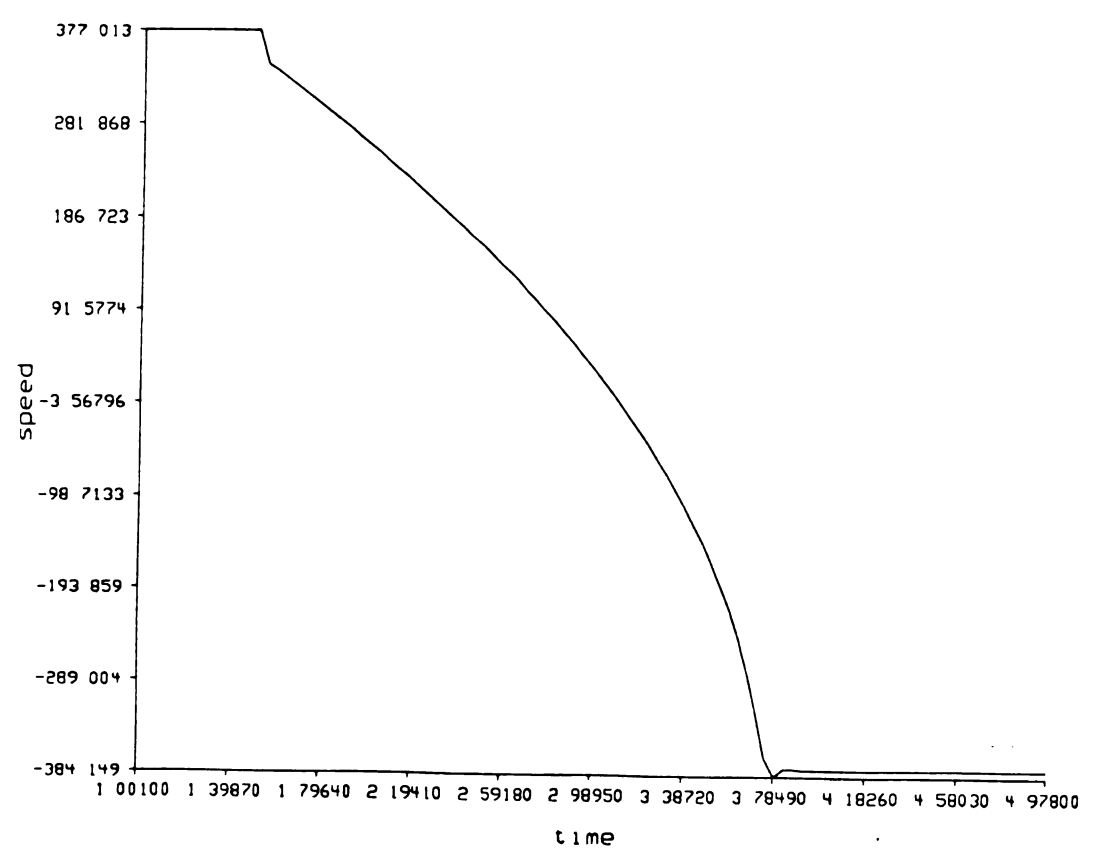


Fig.36 Speed reversal of speed from 377 to -377 rad/sec

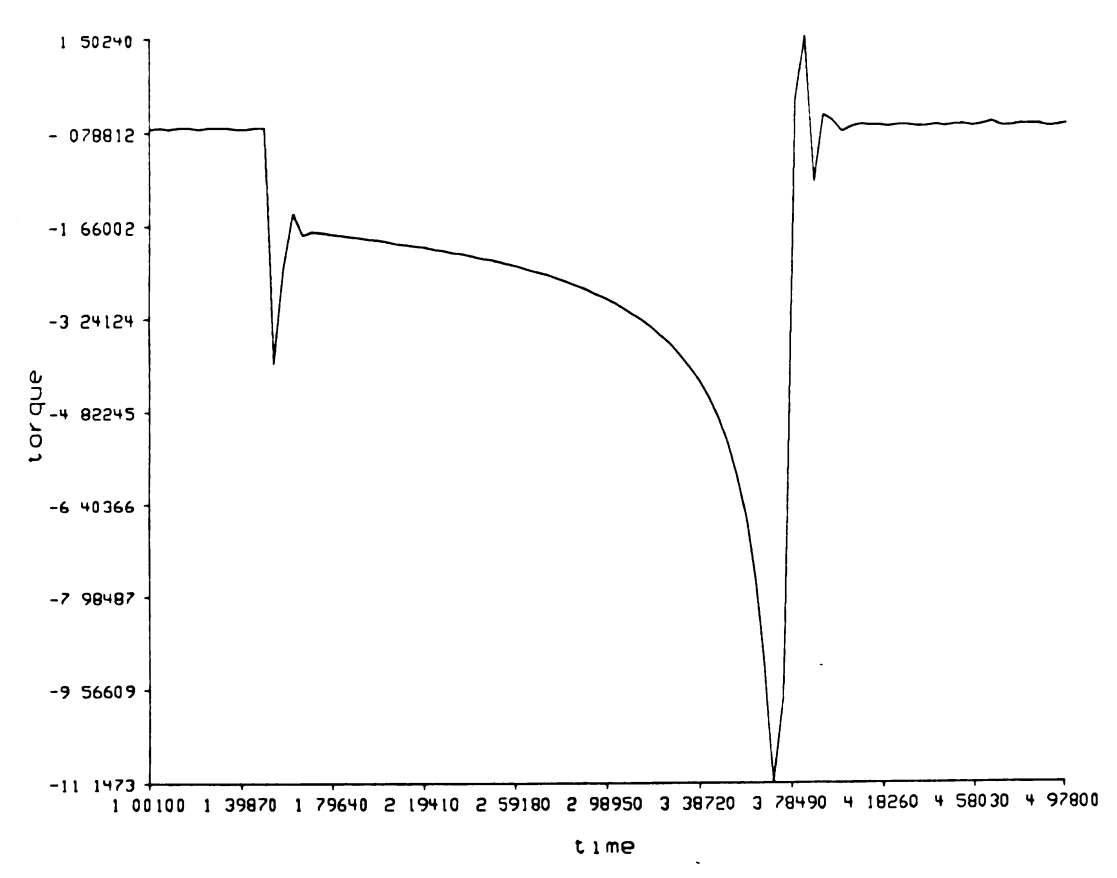


Fig. 37 Speed reversal of torque from 377 to -377 rad/sec

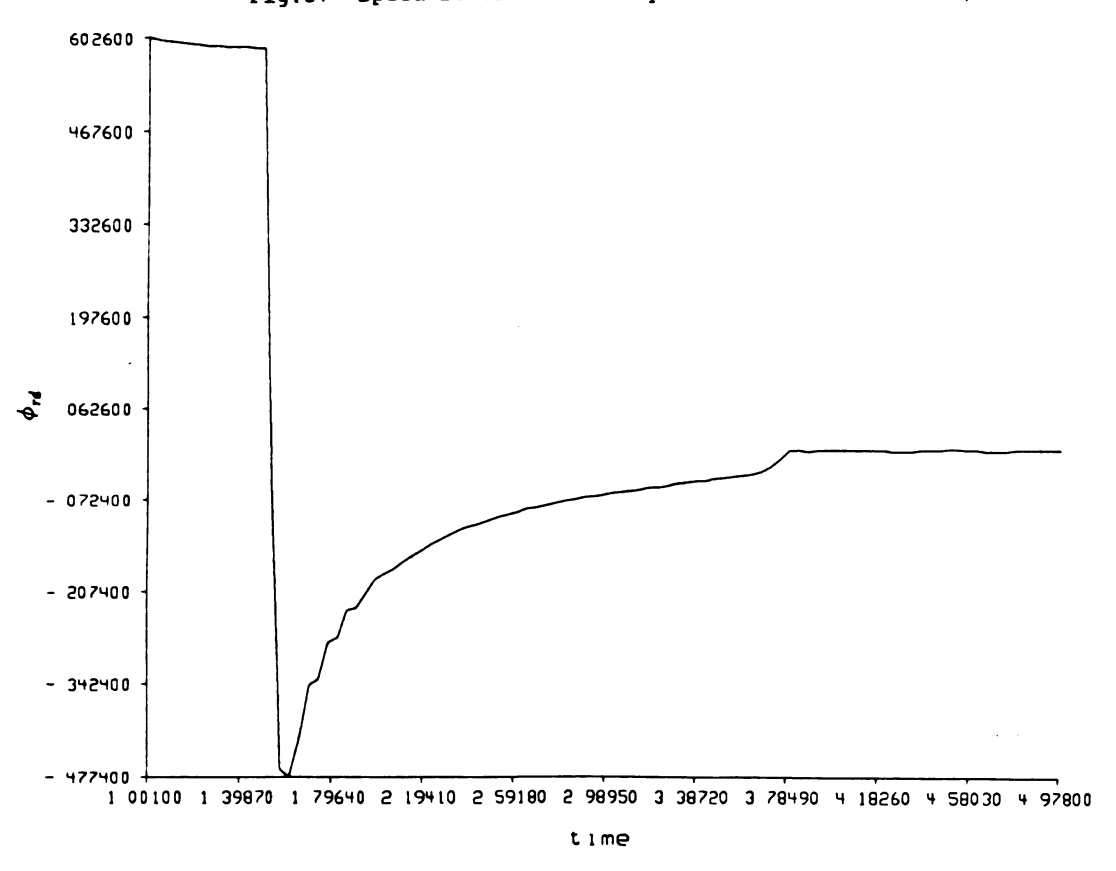
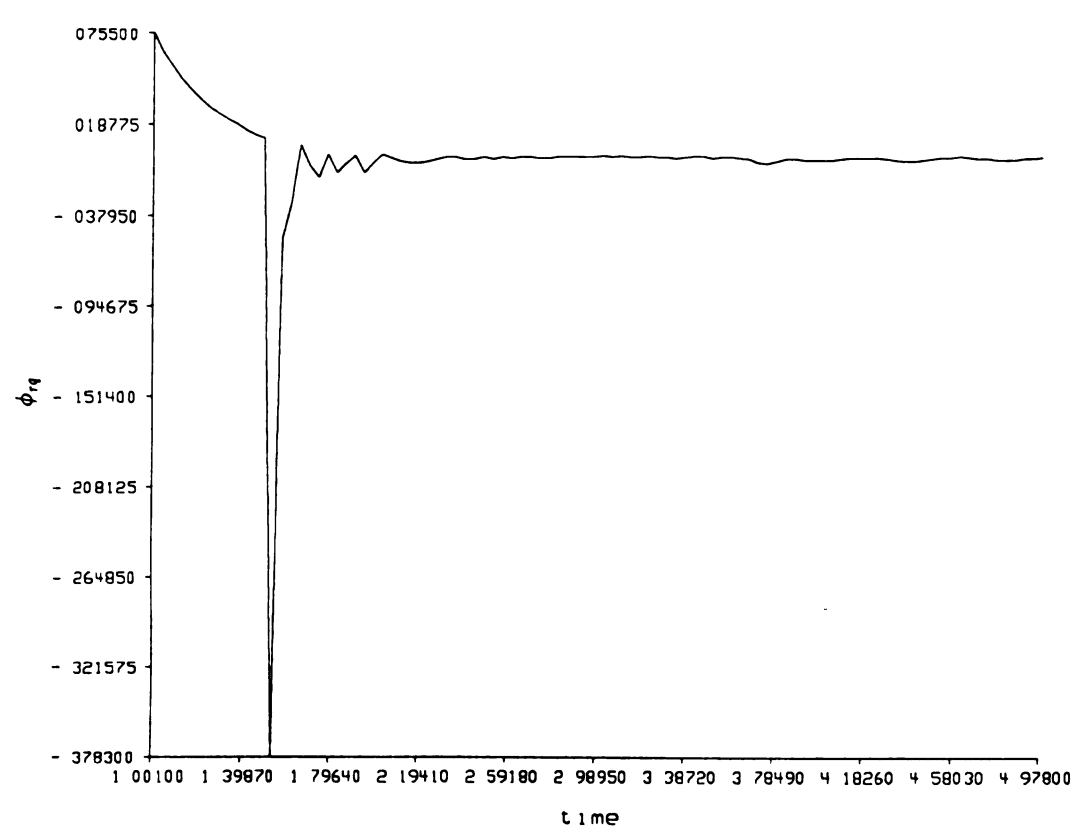


Fig.38 Speed reversal of d-axis rotor flux from 377 to -377 rad/sec



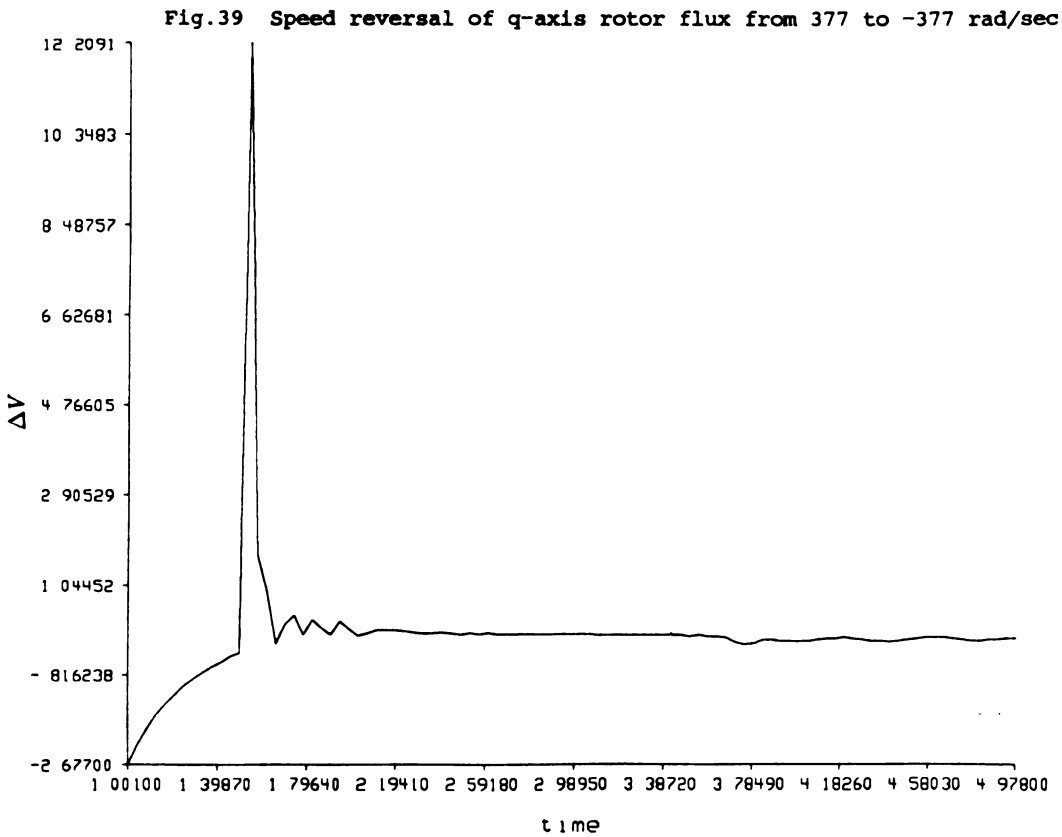


Fig.40 Speed reversal of flux compensation from 377 to -377 rad/sec

9.2 CONCLUSIONS

A field-oriented control (vector control) scheme for an induction machine without speed sensor has been studied along with a PWM method for a three phase inverter.

The proposed drive system allows a high performance speed control that uses only current sensors, thereby eliminating the speed sensor.

In this scheme, deviation of the rotor flux influences the stability and accuracy of the control system. For this reason, compensation for flux deviation was developed. Its effectiveness was verified by digital simulations.

The simulation results verified that the speed and torque control is performed with good dynamic and robust state.

REFERENCES

- 1. W.Leonhard and C.Norby, "Field-oriented control of a standard AC motor using microprocessor", IEEE Trans.on IAS., vol.IA-16, No.2, 1980, pp.186-192.
- 2. R.Joetten and G.Maeder, "Control methods for good dynamic performance induction motor drive based on current and voltage as measured quantities", IEEE Trans.IA-19, No.3, 1983, pp356-362.
- 3. S.Sathikumar and J.Vithayathil, "Digital simulation of field-oriented control of induction machine", IEEE Trans. on Industrial Electronics, vol. IE-31.No.2.1984.
- 4. T.Okuyama, N.Fujimoto, T.Matsui and Y.Kubota, "A high performance speed control scheme of induction motor without speed and voltage sensors", Conference Record, IEEE-IAS. Annual meeting, 1986, pp. 106-111.
- 5. W.Leonard, "Control of electrical drive", Springer-Verlag, 1985.
- 6. K.Lizuka, H.Uzuhashi, M.Kano, T.Endo and K.Mohri, "Microcomputer control of sensorless brushless motor", IEEE Trans. on IAS, vol. IA-21, No. 4, 1985.
- 7. K.Kubo, M. Watanabe, T.Ohmae and K.Kamiyama, "A fully digitalized speed regulator using multi-microprocessor system for induction motor drive", IEEE Trans. IA-21, NO.4, 1985.
- 8. S.Legowski and A.M.Trzynadlowski, "Incremental method of pulse width modulation for three phase inverters", Conf. Rec. 1986 Annual meeting. IEEE IAS, pp.593-600, 1986.
- 9. B.K.Bose and H.A.Sutherland, "A high performance pulse width modulator for an inverter-fed drive system using a microcomputer", IEEE, Trans.IA-19, NO.2, 1983.

- 10. Y.H.Kim and M.Ehsani, "An algebraic algorithm for microcomputer based(direct) inverter pulse width modulation", Conf. Rec. Annual meeting, IEEE, IAS. pp.586-592, 1986.
- 11. I.Boldin and S.A.Nasar, "Electrical machine dynamics", Macmillan publishing company, 1986.
- 12. R.A.Pearman, "Power electronics", Reston publishing company, Inc. 1980.
- 13. B.H.Bose, "Power electronics and AC drives", Prentice Hall, 1986.
- 14. Benjamin.C.Kuo, "Automatic control systems", 5th edition, Prentice Hall, 1987.

MICHIGAN STATE UNIV. LIBRARIES
31293005509785